Journal of Environmental Chemical Engineering 13 (2025) 115465

Contents lists available at ScienceDirect

Journal of Environmental Chemical Engineering

journal homepage: www.elsevier.com/locate/jece

Ozone injection system based on NETmix technology for quaternary treatment of urban wastewater

Mateus Mestriner Pituco [a,b], Paulo H. Marrocos [a,b], Sandra Méndez [c], Rosa Montes [c], Rosario Rodil [c], Francisca C. Moreira [a,b], Vítor J.P. Vilar [a,b,*]

[a] LSRE-LCM – Laboratory of Separation and Reaction Engineering - Laboratory of Catalysis and Materials, Faculty of Engineering, University of Porto, Rua Dr. Roberto Frias, Porto 4200-465, Portugal
[b] ALiCE – Associate Laboratory in Chemical Engineering, Faculty of Engineering, University of Porto, Rua Dr. Roberto Frias, Porto 4200-465, Portugal
[c] Department of Analytical Chemistry, Nutrition and Food Sciences, Institute of Research on Chemical and Biological Analysis (IAQBUS), Universidade de Santiago de Compostela, Constantino Candeira S/N, Santiago de Compostela 15782, Spain

ARTICLE INFO

Keywords:
Ozonation
Contaminants of emerging concern
Static mixer
Gas-liquid mass transfer
Ozone absorption rate

ABSTRACT

An innovative high-intensity static mixer technology, known as NETmix, was applied as an ozone (O_3) gas injection system to promote the quaternary treatment of urban wastewater (UWW), focusing on the elimination of contaminants of emerging concern (CECs). The NETmix network with an exclusive geometry boosts mass transfer rates and rapidly develops an O_3-rich stream to react with CECs. The mixer operated in continuous mode promotes a rapid gas (O_3)–liquid (water) dissolution. The ozonation process' performance was evaluated for the abatement of 19 CECs spiked (10 μg dm^{-3} each) in demineralized water and two tertiary-treated UWW matrices, coming from (i) a secondary settler tank after a conventional activated sludge and (ii) the outlet of a membrane biological reactor (MBR). In addition, the ozonation system was tested for removing a broad range of CECs at natural trace levels from the UWW matrix coming from the MBR. In the realistic wastewater contamination scenario, a maximum transferred O_3 dose of 1.28 g_{O_3} g_{DOC}^{-1} and 0.76 g_{O_3} g_{DOC}^{-1} resulted in removal values ≥80% for 12 out of the 19 spiked CECs from the secondary settler tank, and 9 out of the 19 spiked CECs from the post-MBR treatment, respectively, at a very short hydraulic residence time (55 s). Moreover, removals ≥80% were attained for 22 out of 25 CECs detected in the effluent from the MBR, applying a specific O_3 dose of 0.6 g_{O_3} g_{DOC}^{-1}. The enhanced ozone-water mass transfer provided by the NETmix technology enabled high removal efficiencies for CECs.

1. Introduction

Classical operations using standard biological treatments are not able to efficiently remove contaminants of emergent concern (CECs – e.g., pharmaceuticals, endocrine-disrupting chemicals, synthetic and natural hormones, personal care products, surfactants, pesticides, industrial additives, among others) from urban wastewater (UWW) [1–3]. These contaminants have been detected frequently in treated urban wastewater at levels ranging from a few ng dm^{-3} to a few hundred μg dm^{-3} [4–6]. Recently, the European Commission, following the Circular Economy Action Plan (UN 2030 Agenda), approved a revised Urban Wastewater Treatment Directive (2022/0345/COD). This revised Directive established standards for CECs removal in urban WWTPs (minimum percentage of removal of 80%) and emphasized the widespread reuse of treated effluents [7]. Therefore, a quaternary treatment in WWTPs has become a mandatory step to improve the effluent quality for ecosystem and human health protection [1,8,9].

Ozone (O_3), a strong oxidant and effective disinfectant commonly used in drinking water, has been increasingly applied to upgrade quaternary treatment systems of urban wastewater treatment plants (WWTPs) [8,10–12]. Several works have proven the high ability of ozonation technology incorporated into full-scale urban WWTPs to oxidize CECs and to prevent the dissemination of potentially harmful bacteria (i.e., antibiotic-resistant bacteria and genes – ARB&ARGs) into the environment [5,13–16]. Molecular O_3 (E° = 2.07 V vs. SHE–-standard hydrogen electrode) can react swiftly and selectively with electron-rich molecules such as unsaturated and aromatics compounds,

* Corresponding author at: LSRE-LCM – Laboratory of Separation and Reaction Engineering - Laboratory of Catalysis and Materials, Faculty of Engineering, University of Porto, Rua Dr. Roberto Frias, Porto 4200-465, Portugal
E-mail address: vilar@fe.up.pt (V.J.P. Vilar).

https://doi.org/10.1016/j.jece.2025.115465
Received 20 August 2024; Received in revised form 31 December 2024; Accepted 14 January 2025
Available online 16 January 2025

Nomenclatures

$[O_3]$	Dissolved ozone concentration at time t (g m^{-3} or M)
$[O_3^*]$	Equilibrium dissolved ozone concentration (g m^{-3} or M)
$[O_3]_G$	Gas-phase ozone concentration (g Nm^{-3})
$[O_3]_L$	Outlet dissolved ozone concentration at steady-state (g m^{-3} or M)
δ	Liquid film thickness (m)
a	Specific interfacial area (m^2 m^{-3})
AOD	Applied ozone dose (g m^{-3} or g_{O_3} g_{DOC}^{-1})
C_0	CECs concentration in the feed liquid stream (μg dm^{-3} or M)
$CsOD$	Consumed ozone dose (g m^{-3} or g_{O_3} g_{DOC}^{-1})
D_{O3}	Diffusion coefficient of ozone in the liquid phase (m^2 s^{-1})
E	Enhancement factor (dimensionless)
H	Henry constant (dimensionless)
Ha	Hatta number (dimensionless)
IOD	Immediate ozone demand (g m^{-3})
k	Chemical reaction rate constant (M^{-1} s^{-1})
k_d	Ozone decay kinetic constant (s^{-1})
k_L	Liquid phase individual mass transfer coefficient (m s^{-1})
k_La	Liquid phase volumetric mass transfer coefficient (s^{-1})
k_{UVA254}	Rate of UVA_{254} reduction (M^{-1})
η	Transfer efficiency (%)
N_{O3}	Gas-liquid mass transfer rate (M s^{-1})
Q_G	Gas volumetric flowrate (Ndm^3 h^{-1})
Q_L	Liquid volumetric flowrate (dm^3 h^{-1})
t	Time (s)
τ	Liquid phase residence time (s)
τ_{NETmix}	NETmix liquid phase residence time (s)
τ_{CC}	Contact column liquid phase residence time (s)
τ_{system}	System liquid phase residence time (s)
TOD	Transferred ozone dose (g m^{-3} or g_{O_3} g_{DOC}^{-1})
UVA_{254}	Ultraviolet Absorbance at 254 nm (cm^{-1})

Subscripts

O_3	Associated with ozone species
$^{\bullet}OH$	Associated with hydroxyl radicals
L	Indication of the liquid phase
G	Indication of the gas phase
0	Designates an initial condition or conditions at reactor inlet

Superscripts

in	Refers to inlet gas stream
out	Refers to outlet gas stream

olefins, and neutral/tertiary amines, while it can also generate hydroxyl radicals ($^{\bullet}OH$, E° = 2.87 V vs. SHE) which is less selective but more reactive [16–18]. As such, several compounds, which are theoretically very resistant to O_3, can still be oxidized due to indirect oxidation involving $^{\bullet}OH$ [19,20]. Nevertheless, a key factor that requires improvement to facilitate the massive penetration of ozonation processes in the wastewater treatment sector is the injection technique to transfer the O_3 gas stream into water [21,22]. As O_3 dissolved in water is exceedingly unstable, maintaining a significant O_3 residual in a wastewater stream is difficult [23]. Consequently, O_3 injection methods with poor gas-liquid mass transfer rates result in higher O_3 dose requirements and a considerable footprint to promote the disinfection/oxidation treatment [16,22,24].

O_3-water injection methods consist of dispersing the O_3 gas stream into the liquid phase via (i) fine bubble diffusers (FBD) or (ii) injection of a concentrated O_3 solution via a sidestream [12,22,25,26]. In FBD, the O_3 mass transfer (i.e., dissolution of O_3 gas in water) and mixing/-reaction are carried out simultaneously in bubbling columns or multi-chamber contactors. However, some disadvantages limit the employment of this typical injection system, such as high ozone supply demands, prolonged contact time in the reaction tank, and the large equipment size [16,27,28]. On the other hand, sidestream injection (SSI) systems have been gaining popularity as one of the most promising techniques to overcome the FDB limitations [25]. In SSI, a sidestream water flow (a stream containing 3–5% of the total influent flow) is supplemented with O_3 gas through a venturi or static mixers, and mixed back into the main water flow to attain a desired O_3 dose at the mixing/reaction zone of the multi-chamber contact tank [12,29]. This configuration minimizes the ozone dose and residence time required for CECs oxidation and disinfection, compared to FBD systems (e.g., 5 – 10 min in SSI *vs.* 15 – 30 min in FBD systems [21,22]), associated with the larger O_3 mass transfer rate, favoring the O_3 dissolution [22,30–32].

In a previous work, Pituco et al. [33] proposed a device able to provide high-mixing intensity and rapid O_3 gas dissolution based on the innovative micro/meso-structured NETmix static mixer. The NETmix technology comprises a network of mixing chambers interconnected by transport channels, where the chambers work as perfectly mixed stirred tanks and the channels operate as ideal plug flow devices [34,35]. Its exclusive geometry provides unique benefits, including the possibility of controlling the residence time and intensity of mixing, and the capability to operate under lower gas-liquid pressure drops than other static mixers (e.g., screen-type and Lightnin static mixers) [35–37]. As a result, better control of the mass transfer is enabled, thus broadening the possible applications of this technology [38,39]. The intrinsic ability of the NETmix to improve mixing processes has led to volumetric gas-liquid mass transfer coefficient (k_La) values (0.83 – 2.46 s^{-1}) that outperformed by one to two orders of magnitude the main technologies industrially used in gas injection systems for ozonation processes (e.g., stirred tanks, bubble columns equipped with diffusers, venturis or membrane reactors) [33]. Likewise, the NETmix technology has demonstrated its efficiency for water treatment systems with mass transfer limitations, such as photocatalysis and electrochemical processes [40–44].

Therefore, this work aims to deepen the application of the NETmix technology as a novel O_3 gas injection system for quaternary treatment of urban wastewater. The performance of the ozonation process was evaluated for the removal of 19 CECs, selected based on the occurrence and persistence in river basins and WWTPs effluents in Northern Portugal and Spain [4,6,45,46]. These compounds were spiked in demineralized water and tertiary-treated UWW (10 μg dm^{-3} each). The influence of the effluent quality on the ozonation efficiency was assessed based on different UWW matrices collected in two WWTPs, coming from (i) the secondary settler tank after a conventional activated sludge process and (ii) a post-treatment membrane biological reactor. In addition, the ozonation system was applied to remove a broad range of CECs at realistic trace levels (without fortification) from the post-MBR effluent. The effect of different experimental parameters on CECs removal was examined, including the applied and transferred O_3 dose (*AOD* and *TOD*, respectively), gas-phase O_3 concentration ($[O_3]_G^{in}$) and gas flow rate (Q_G), and hydraulic residence time (HRT).

2. Materials and methods

2.1. Water matrices

CECs removal was evaluated using three distinct water matrices: a

synthetic water matrix (SW) comprised of demineralized water (provided by reverse osmosis system; Panice®) and two real urban wastewater matrices denoted as UWW1 and UWW2. These water matrices were contaminated with 19 CECs (10 μg dm^{-3} each), as indicated with '†' in Table 1. The selection of these compounds was based on their occurrence and persistence in river basins and WWTPs effluents from the northern region of Portugal and Galicia (Spain), as reported in previous studies [4,6,45,46].

The 19 target CECs included Losartan, 17α-Ethynylestradiol, Acesulfame K, Diethyltoluamide, Bisoprolol, 17β-Estradiol, Carbamazepine, Atenolol, Carbamazepine 10,11-epoxide, Diuron, Heptafluorobutyric acid, Irbesartan, Diclofenac, Pentadecafluorooctanoic acid, Nonafluoro-1-butanesulfonic acid, Melamine, Valsartan, Trifluoromethanesulfonic acid, and Saccharin. All reagents were of analytical grade (>98%) and supplied by Sigma-Aldrich (Steinheim, Germany). A stock solution (1 g dm^{-3}) was prepared in ultrapure water (Millipore Direct-Q®, 18.2 MΩ cm^{-1} at 25°C) or methanol (Merck), stored in glass vials and protected from light at 4°C.

2.1.1. Urban wastewater

The real wastewater matrices, UWW1 and UWW2, were collected after the tertiary treatment process at two urban WWTPs located in Northern Portugal. Specifically, UWW1 was collected downstream of a WWTP secondary settling tank responsible for the supply of a population of 150,000 inhabitants ($WWTP_I$), whereas UWW2 was collected from a pilot membrane biological reactor (MBR) installed within a WWTP serving a population of 170,000 inhabitants ($WWTP_{II}$). The respective physicochemical properties are summarized in Table 2. The UWW matrices, coming from two distinct biological treatment processes, exhibited broad variation in their main quality physicochemical parameters (e.g., chemical oxygen demand, dissolved organic and inorganic carbon, and turbidity). These differences were sufficiently significant to consider valuable the assessment of the ozonation process's performance (e.g., ozone demand) in the removal of CECs.

2.1.2. CECs measured in a screening campaign

The analyzes of CECs through the screening campaign were performed in samples taken at $WWTP_{II}$ for 19 target contaminants (indicated by '‡' in Table 1). In summary, the sewage consisted of 80% domestic wastewater and 20% industrial wastewater, which were potential sources of specific micropollutants. The wastewater treatment included pre-treatments (grit removal and screening), primary and secondary clarifiers, biological activated sludge (anoxic and aerated) treatment, a pilot MBR system, and a UV disinfection process.

During the campaign, 24-hour composite samples were collected at i) influent of the $WWTP_{II}$ after grit removal and screening (raw wastewater) and ii) effluent of the $WWTP_{II}$ after UV disinfection (treated wastewater). Also, samples were collected at the inlet and outlet of the pilot MBR system. Specifically, the wastewater effluent collected at the outlet of the MBR (post-MBR treatment – UWW2 matrix) was analyzed in the screening campaign for 32 target CECs, all detailed in Table 1. Out of these target micropollutants, 25 contaminants surpassed the limit of

Table 1
Selected CECs along with respective apparent second-order reaction rate constant with ozone (k_{O3}) and •OH ($k\bullet_{OH}$).

Contaminant		Contaminant class	Molecular formula	k_{O3} ($M^{-1}s^{-1}$)	Ref.	$k\bullet_{OH}$ ($M^{-1}s^{-1}$)	Ref.
Pharmaceuticals							
Amantadine‡	**AMT**	Antiviral drug	$C_{10}H_{17}N$	3.45	[47]	6.31×10^{9}	[48]
Amisulpride‡	**ASPD**	Antipsychotic	$C_{17}H_{27}N_3O_4S$	1.50×10^{5}	[14]	Unknown	-
Atenolol†‡	**ATNL**	Beta blocker	$C_{14}H_{22}N_2O_3$	1.70×10^{3}	[49]	8.00×10^{9}	[49]
Bisoprolol†	**BSPL**	Beta blocker	$C_{18}H_{31}NO_4$	1.83×10^{4}	[50]	Unknown	-
Carbamazepine†‡	**CBZ**	Anticonvulsant	$C_{15}H_{12}N_2O$	3.00×10^{5}	[51]	8.80×10^{9}	[51]
Diclofenac†	**DCF**	Anti-inflammatory	$C_{14}H_{11}Cl_2NO_2$	1.00×10^{6}	[51]	7.50×10^{9}	[51]
Flecainide‡	**FLE**	Antihypertensive	$C_{17}H_{20}F_6N_2O_3$	1.30×10^{5}	[52]	Unknown	-
Irbesartan†‡	**ISTN**	Antihypertensive	$C_{25}H_{28}N_6O$	24	[14]	1.00×10^{10}	[14]
Lamotrigine‡	**LAM**	Anticonvulsant	$C_9H_7Cl_2N_5$	4	[53]	2.10×10^{9}	[53]
Losartan†	**LSTN**	Antihypertensive	$C_{22}H_{23}ClN_6O$	2.10×10^{5}	[14]	Unknown	-
Metformin‡	**MET**	Antidiabetic	$C_4H_{11}N_5$	1.2	[54]	1.40×10^{9}	[55]
Sulpiride‡	**SPD**	Antipsychotic	$C_{15}H_{23}N_3O_4S$	2.50×10^{4}	[56]	Unknown	-
Tramadol‡	**TRA**	Antipyretic	$C_{16}H_{25}NO_2$	2.20×10^{3}	[57]	6.30×10^{9}	[57]
Tiapride‡	**TPD**	Antipsychotic	$C_{15}H_{24}N_2O_4S$	Unknown	-	Unknown	-
Valsartan†	**VSTN**	Antihypertensive	$C_{24}H_{29}N_5O_3$	38	[58]	1.00×10^{10}	[58]
Venlafaxine‡	**VEN**	Antidepressant	$C_{17}H_{27}NO_2$	1.30×10^{3}	[59]	8.80×10^{9}	[55]
Endocrine disrupting compounds							
17α-Ethynylestradiol†	**EE2**	Hormonal contraceptive	$C_{20}H_{24}O_2$	3.00×10^{6}	[51]	9.80×10^{9}	[51]
17β-Estradiol†	**E2**	Hormone	$C_{18}H_{24}O_2$	2.21×10^{6}	[60]	5.77×10^{9}	[60]
Pharmaceutical metabolites							
Carbamazepine 10,11-epoxide†	**CBZ-E**	Drug metabolite	$C_{15}H_{12}N_2O_2$	Low[a]	[61]	Low[a]	[61]
O-desmethylvenlafaxine‡	**ODV**	Drug metabolite	$C_{16}H_{25}NO_2$	High[a]	[62]	Unknown	-
Biocides — pesticides							
Diethyltoluamide†‡	**DEET**	Insecticide	$C_{12}H_{17}NO$	0.1	[63]	4.95×10^{9}	[64]
Diuron†‡	**DRN**	Herbicide	$C_9H_{10}Cl_2N_2O$	28.2	[60]	6.23×10^{9}	[60]
Terbutryn‡	**TBT**	Algicide	$C_{10}H_{19}N_5S$	Unknown	-	Unknown	-
Food additives							
Acesulfame K†‡	**AC-K**	Artificial Sweetener	$C_4H_4KNO_4S$	88	[29]	4.55×10^{9}	[29]
Caffeine‡	**CAFF**	Stimulant	$C_8H_{10}N_4O_2$	6.50×10^{2}	[65]	5.90×10^{9}	[66]
Saccharin†	**SAC**	Artificial Sweetener	$C_7H_5NO_3S$	4.0×10^{-1}	This work	1.56×10^{9}	[67]
Other common chemicals							
Melamine†	**MEL**	Flame retardant/ Industrial chemical	$C_3H_6N_6$	Unknown	-	1.00×10^{4}	[68]
Tris (2-chloroisopropyl) phosphate‡	**TCPP**	Industrial chemical	$C_9H_{18}Cl_3O_4P$	<2	[69]	7.00×10^{8}	[69]
Short-chain perfluoroalkyl substances (PFAS)							
Heptafluorobutyric acid†	**PFBA**	Industrial chemical	$C_4HF_7O_2$	Unknown	-	Unknown	-
Pentadecafluorooctanoic acid†	**PFOA**	Industrial chemical	$C_8HF_{15}O_2$	Unknown	-	$\leq 1\times10^{5}$	[70]
Perfluorobutane sulfonate†	**PFBS**	Industrial chemical	$C_4HF_9O_3S$	Unknown	-	Unknown	-
Trifluoromethanesulfonic acid†	**TFMS**	Industrial chemical	CHF_3O_3S	Unknown	-	$\leq1\times10^{5}$	[71]

† 19 target CECs selected for contamination of water matrices (SW, UWW1, and UWW2);
‡ 19 target CECs analyzed in the screening campaign;
[a] Estimated reactivity.

Table 2
Physicochemical properties of both wastewater samples collected downstream of the tertiary treatment in two WWTPs (UWW1 – settling tank effluent, and UWW2 – post-MBR effluent) and after ozonation process.

Parameter (units)	UWW1	O_{3-UWW1} [a]	UWW2	O_{3-UWW2} [a]
Conductivity (μS cm^{-1})	1095	-	618	507
pH	7.4	7.7	7.6	7.4
Temperature (°C)	17.6	21.1	18.4	19.2
Turbidity (NTU)	3.7	1.2	1.6	0.5
Total Suspended Solids, TSS (g m^{-3})	13.0	4.0	12.2	5.0
Chemical Oxygen Demand, COD (g_{O2} m^{-3})	70.1	58.4	22.3	13.6
Total Dissolved Carbon (g m^{-3})	82.1	43.3	25.7	23.7
Dissolved inorganic carbon (g m^{-3})	66.4	28.8	15.7	13.9
Dissolved organic carbon (g m^{-3})	15.7	14.5	10.0	9.7
Ultraviolet Absorbance at 254 nm (UVA_{254})	0.273	0.141	0.204	0.116
Specific Ultraviolet Absorbance (SUVA, m^3 g^{-1} m^{-1})	1.74	0.972	2.04	0.701
Sodium, Na^+ (g m^{-3})	112.8	111.3	67.8	66.2
Ammonium, NH_4^+ (g m^{-3})	54.8	24.3	1.6	1.1
Potassium, K^+ (g m^{-3})	24.6	23.1	24.4	24.6
Magnesium, Mg^{2+} (g m^{-3})	7.7	8.4	7.6	7.4
Calcium, Ca^{2+} (g m^{-3})	31.8	28.1	48.1	47.5
Chloride, Cl^- (g m^{-3})	141.7	135.3	87.8	85.7
Nitrite, NO_2 (g N m^{-3})	0.06	0.05	1.57	1.55
Sulfate, SO_4^{2-} (g m^{-3})	58.9	58.2	69.1	64.7
Nitrate, NO_3 (g m^{-3})	23.6	85.0	87.7	83.4
Phosphates, PO_4^{3-} (g m^{-3})	18.2	19.8	17.5	16.8

[a] Applied ozone dose = 2.0 $g_{O_3} g_{DOC}^{-1}$

quantification (LOQ). These 25 CECs detected in the UWW2 were subsequently evaluated for their removal efficiencies during ozonation.

2.2. Rate constants for the reaction of CECs with ozone and hydroxyl radicals

Table 1 summarizes the apparent second-order reaction rate constants for the reactions of 32 target CECs with ozone (k_{O3}) and hydroxyl radicals ($k_{\bullet OH}$) reported in the literature (at circumneutral pH conditions). Among the relevant contaminants with unknown kinetic data, this work focused on determining the k_{O3} of Saccharin (SAC), an important compound continuously detected in real wastewater matrices. The kinetic reactions were performed in *semi*-batch conditions, and the k_{O3} of $(2.4\pm0.1)\times10^{-2}$ M^{-1} s^{-1} and $(4.0\pm0.1)\times10^{-1}$ M^{-1} s^{-1} were determined at pH 2 and 7, respectively (see experimental procedure in the Chapter S1 of the Supplementary Material).

2.3. Analytical determinations

The respective analytical methodologies utilized to determine the physicochemical parameters summarized in Table 2 are detailed in Table S1 of the Supplementary material. The analyses of CECs in liquid samples were performed in a ultra-high performance liquid chromatography (Acquity UPLC®) interfaced to a XEVO TQD® triple quadrupole mass spectrometer (LC-MS/MS) equipped with an electrospray ionization (ESI) from Waters (Milford, MA, USA). The quantification was done according to the standard addition method based on standards prepared in SW and UWW matrices, and by directly injecting the samples. Further details on the method's performance parameters and chromatograms may be found in Presumido et al. [46]. Specifically, in this work, the analytical methodology's performance was reassessed for SW and UWW matrices contaminated with the 19 CECs, such that the determined limit of quantification is shown in Table S2. For the CECs measured in the screening campaign (described in Section 2.1.2), the wastewater samples were processed through the procedure provided by Montes et al. [4]. Detailed information regarding these concentrations of CECs and method quantification limit is provided in Table S3.

2.4. Experimental setup and procedure

2.4.1. NETmix static mixer

A detailed description of the NETmix static mixer has previously been given by Pituco et al [33] and its schematic is depicted in Fig. 1. Briefly, it consists of a network generated by the repetition of unit cells, in which each unit cell is formed by one cylindrical chamber connected to two inlet and two outlet prismatic half-channels oriented at a 45º angle from the main flow direction (Fig. 1 – left). In this work, the NETmix comprised a stainless-steel structure containing a rear plate on which the network of unit cells was machined, with cylindrical chambers of 6.5 mm diameter, as well as prismatic channels of 1 mm width and 2 mm length. The unit cell's depth was 3 mm and the network had a total of 29 chamber rows. Despite these small characteristic dimensions, the low suspended solids content in both UWW matrices (see Table 2) led to no indication of fouling/clogging in the NETmix network. The rear plate was sealed by a frontal plate containing a window of borosilicate glass slab (5.0 mm thickness and cut-off at 190 mm) so that a visualization of the flow was enabled. O-rings and fixing screws were used to seal both plates (Fig. 1 – right). The reactor has eight inlets (four located at the front, and four at the rear), responsible for fluid injection into eight inlet chambers placed at the top of the static mixer. In addition, it also has eight outlet chambers placed at the bottom of the network.

2.4.2. Evaluation of CECs removal

Fig. 2a illustrates the experimental apparatus used for the ozonation tests, whereas Fig. 2b displays a photograph of NETmix reactor (left) and highlights the gas-liquid flow inside a unit cell of the mixer (right).

O_3 gas was produced from pure oxygen (O_2, 99.995 wt% supplied by Alphagaz™) by a corona discharge O_3 generator (BMT 802 N, Messtechnik, Germany). The input gas flowrate (Q_G) was regulated using a digital mass flow meter (Alicat Scientific), and the power input of the O_3 generator was adjusted to achieve the required O_3 concentration ($[O_3]_G^{in}$ = 30–104 g Nm^{-3}). The inlet and outlet gas-phase O_3 concentration ($[O_3]_G^{in}$ and $[O_3]_G^{out}$, respectively) were monitored using a UV-photometric O_3 analyzer (BMT 964), located downstream of a gas dehumidifier (BMT DH3b). A heated catalyst (BMT Heated-Cat) was used to destroy the remaining O_3 before exhaustion.

The NETmix was set vertically, and the O_3 gas and liquid streams were injected simultaneously into the mixer in a co-current downward flow. Both liquid and gas feed streams were independently linked to two flow distributors - composed of stainless-steel - containing four outlets each, alternately coupled to the eight inlet chambers of the NETmix network. SW, UWW1 or UWW2 was introduced into the NETmix from a jacketed vessel (volume of 5.0 dm^3) at a liquid flowrate (Q_L) set by a flowmeter (Omega™) using a Ismatec gear pump (BVP-Z; MI0016). The reaction temperature was maintained at 20 ± 1ºC by a temperature controller (Lab. Companion, RW-0525G) attached to the jacketed vessel. At the bottom of the mixer, another flow distributor, with eight inlets and one outlet, collected the static mixer gas-liquid outlet stream. Subsequently, this stream was fed to the bottom inlet of a cylindrical contact column (75 mm internal diameter × 450 mm height, net volume of 1.5 dm^3) for gas-liquid separation and to provide the contact time required for dissolved O_3 reaction with CECs. The pH of the SW, UWW1, and UWW2 matrices was kept at circumneutral conditions (6.8±0.2, 7.4 ±0.3, and 7.6±0.1, respectively). O_3-resistant fittings and Teflon (PTFE) tubes were used for all connections. The NETmix reactor was machined in 316-grade stainless steel, a high-resistance material to ozone-induced corrosion. Liquid samples for the analyses of CECs and dissolved O_3 concentration ($[O_3]_L$) were taken from the sampling port at the NETmix reactor outlet (SP1, Fig. 2) or at the upper outlet of the contact column (SP2, Fig. 2) at pre-established periods after the steady-state has been

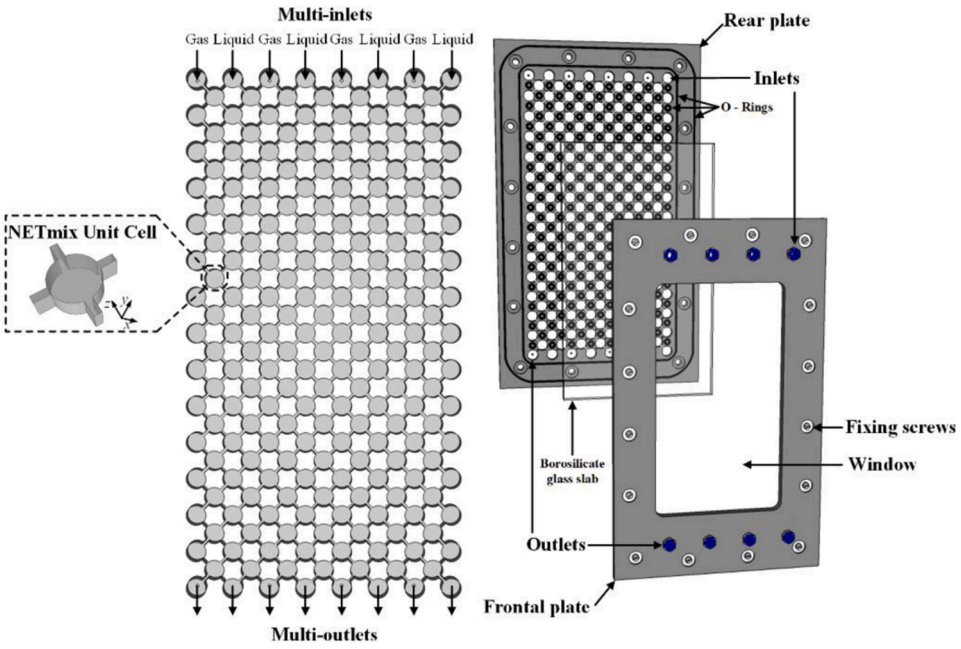

Fig. 1. Sketch-up of the NETmix static mixer (left) and the NETmix reactor disassembled (right).

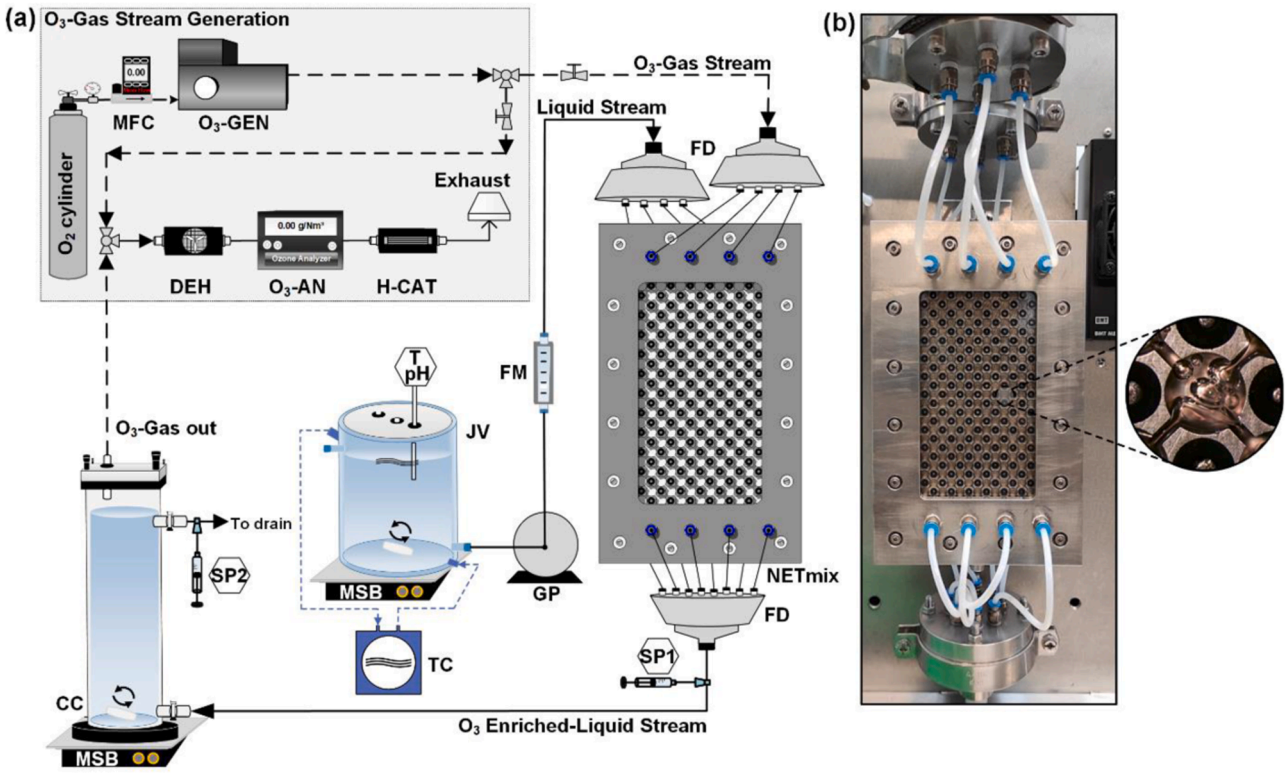

Fig. 2. **(a)** Schematic diagram of the laboratory-scale experimental setup. **(b)** Photographs of the NETmix reactor (left) and gas-liquid flow inside a unit cell of the mixer (right). Legend: **MFC –** mass flow controller; **O_3-GEN –** ozone generator; **DEH –** dehumidifier; **O_3-AN –** ozone analyzer; **H-CAT –** Heated catalyst; **TC –** Temperature controller; **JV –** jacketed vessel; **MSB** – magnetic stir bar; **T, pH –** Temperature and pH sensor; **GP –** gear pump; **FM** – liquid flow meter; **FD –** flow distributor; **SP –** sampling point; **CC** – contact column.

verified. The liquid-phase O_3 concentration was determined according to the indigo colorimetric method [72], in which samples were placed in volumetric glass vials containing a indigo solution; then a Spectroquant Prove 300 UV/vis spectrophotometer (Merk) was used to measure the absorbance at 600 nm wavelength, considering a molar absorptivity of 20,000 M^{-1} cm^{-1}. Whereas, for CECs analysis, the samples were immediately placed in a water bath at 60°C to quench any residual O_3.

The removal percentages of the CECs were calculated from the following expression: Removal $(\%) = 100 \times (1–C/C_0)$, in which C_0 and C are the initial and final concentrations of the targeted contaminant, respectively, provided that the final concentration was above the LOQ. The estimation of parameters regarding the applied (*AOD*),

transferred (*TOD*), and consumed (*CsOD*) ozone doses, considered units of g m^{-3}, were determined using the equations presented by Rakness (2005) [22], as indicated in Eqs. (1)–(4):

$$AOD = \frac{Q_G \times [O_3]_G^{in}}{Q_L} \quad (1)$$

$$TOD = AOD \times \eta \quad (2)$$

$$\eta = \frac{[O_3]_G^{in} - [O_3]_G^{out}}{[O_3]_G^{in}} \quad (3)$$

$$CsOD = TOD - [O_3]_L \quad (4)$$

where *AOD* and *TOD* correspond to the injected ozone dose, and the quantity of applied ozone dose that has successfully been transferred to the liquid phase, respectively; and η is the ozone transfer efficiency. Given that the ozone consumption associated with wastewater effluents is intrinsically influenced by the quantity of dissolved organic matter (DOM), *AOD* and *TOD* were normalized with respect to the dissolved organic carbon concentration (DOC) for the UWW matrices. The conditions of the experiments performed in this work are summarized in Table 3. All experiments were done in continuous mode, where the majority of experiments were conducted with Q_G = 30 Ndm^3 h^{-1} and Q_L = 100 dm^3 h^{-1} (only for the specific tests #1 and #5, Q_L and Q_G were changed, respectively), corresponding to a system liquid phase residence (τ_{system}) around 55 s. τ_{system} results from summing the liquid phase residence time at the NETmix (τ_{NETmix}) and at the contact column (τ_{cc}), represented by Eqs. (5)–(7).

$$\tau_{NETmix} = (1 - \alpha_G) \times \frac{V_{NETmix}}{Q_L} \quad (5)$$

$$\tau_{cc} = \frac{V_{CC}}{Q_L} \quad (6)$$

$$\tau_{system} = \tau_{NETmix} + \tau_{cc} \quad (7)$$

where α_G is the gas hold-up fraction, considered as the gas volume per total volume of the NETmix and calculated according to Pituco et al. [33]; V_{NETmix} is the total volume of the mixer (0.023 dm^3), and V_{CC} is the volume of liquid in the contact column (1.5 dm^3).

3. Results and discussion

3.1. Removal of CECs spiked in synthetic water

3.1.1. Performance of the NETmix reactor for CECs abatement

In order to study the performance of the NETmix reactor on the removal of 19 target CECs, experiments were performed in SW considering the nearly-zero contact time in the NETmix network. A Q_L of 50 dm^3 h^{-1} and 100 dm^3 h^{-1} were applied, corresponding to τ_{NETmix} = 1.02 s and τ_{NETmix} = 0.61 s, respectively. Additionally, Q_G of 30 Ndm^3 h^{-1} and $[O_3]_G^{in}$ of 30 g Nm^{-3} were fixed. The results obtained for removal efficiency under these conditions are depicted in Fig. 3a.

It could be seen that the ozonation process at a relatively low Q_L (50 dm^3 h^{-1}) and τ_{NETmix} of 1.02 s was enough to achieve a satisfactory degradation (≥80% or below LOQ) for at least 5 out of the 19 CECs. Such target degradation improved to 8 CECs when the Q_L was raised to 100 dm^3 h^{-1}, resulting in τ_{NETmix} = 0.61 s. This effect is due to a larger O_3 mass transfer rate in the NETmix reactor when Q_L is increased, resulting in greater degradation for the target CECs (Fig. 3a), although there is a decrease in the applied O_3 dose and residence time. It was demonstrated in a previous work [33] that Q_L was a crucial parameter in the transfer of O_3 to the liquid in the NETmix. By an increase in Q_L, the drag force exerted by the liquid phase on the gas phase when flowing from the chambers to the channels is favored. This phenomenon leads to the reduction of the liquid film thickness or the development of smaller-sized gas bubbles, resulting in a larger interfacial area, and reduced O_3-liquid boundary layer resistance [33].

As O_3 is considerably stable in SW, the transferred O_3 doses were not completely consumed during the very short residence times associated with the NETmix reactor. Theoretically, using larger hydraulic residence times guarantees a maximal consumption of the transferred O_3. Therefore, a contact column was coupled downstream of the NETmix reactor to increase the system's residence time (to 55 s, corresponding to Q_L = 100 dm^3 h^{-1}). In Fig. 3b, it is compared the CECs removal when solely the NETmix reactor (τ_{NETmix} = 0.61 s – test#2, Table 3) is used and when

Table 3
Experimental conditions considered in each test.

Test	Q_G Ndm^3 h^{-1}	Q_L dm^3 h^{-1}	τ s	$[O_3]_G^{in}$ g Nm^{-3}	*AOD* g m^{-3} (g_{O_3} g_{DOC}^{-1})	*TOD* g m^{-3} (g_{O_3} g_{DOC}^{-1})[c]	*CsOD* g m^{-3} (g_{O_3} g_{DOC}^{-1})
SW							
Synthetic water matrix with 19 CECs spiked							
#1	30	50	1.02[a]	30	18.0	6.9	2.7
#2	30	100	0.61[a]	30	9.0	5.6	2.7
#3	30	100	55[b]	30	9.0	5.5	2.8
UWW1							
Wastewater matrix with 19 CECs spiked							
#4	30	100	55[b]	30	9.0 (0.56)	7.0 (0.43)	7.0 (0.43)
#5	45	100	55[b]	40	18.0 (1.15)	11.3 (0.71)	11.3 (0.71)
#6	30	100	55[b]	60	18.0 (1.15)	12.9 (0.81)	12.7 (0.79)
#7	30	100	55[b]	104	31.0 (2.0)	20.3 (1.28)	18.4 (1.16)
UWW2							
Wastewater matrix with 19 spiked CECs							
#8	30	100	55[b]	30	9.0 (0.9)	8.1 (0.27)	8.1 (0.27)
#9	30	100	55[b]	38	12.0 (1.15)	8.9 (0.35)	8.9 (0.35)
#10	30	100	55[b]	50	15.0 (1.5)	10.8 (0.54)	10.8 (0.54)
#11	30	100	55[b]	67	20.0 (2.0)	13.0 (0.76)	13.0 (0.76)
Wastewater matrix without spiked CECs							
#12	30	100	55[b]	30	9.0 (0.9)	7.7 (0.23)	7.7 (0.23)
#13	30	100	55[b]	38	12.0 (1.15)	8.2 (0.30)	8.2 (0.30)
#14	30	100	55[b]	50	15.0 (1.5)	9.6 (0.42)	9.0 (0.36)
#15	30	100	55[b]	67	20.0 (2.0)	11.3 (0.60)	9.3 (0.40)

[a] refers to the τ_{NETmix}
[b] refers to the τ_{system}
[c] *TOD* values shown are corrected for the O_3 demand exerted by nitrite.

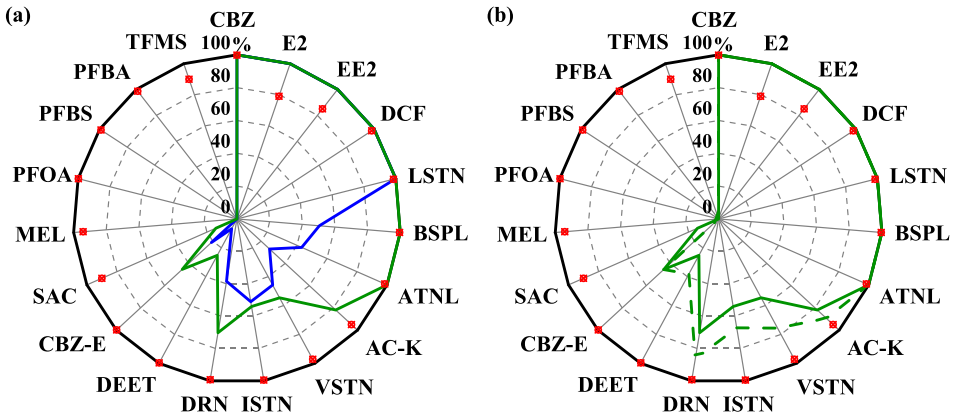

Fig. 3. Removal efficiency (%) related to the 19 spiked CECs in SW (C_0 = 10 μg dm^{-3}) after a treatment time of: **(a)** 1.02 s ( ) and 0.61 s ( ) using only the NETmix reactor; **(b)** 0.61 s ( ) and 55 s ( ) using the coupled NETmix reactor plus contact column system. The red symbol ( ) indicates the limit of quantification (LOQ) of the method.

the NETmix is coupled with the contact column (τ_{system} = 55 s – test#3, Table 3). Enhancements were detected in the removal efficiency of several CECs for the system with a residence time of 55 s, with increases between 1.1 and 1.5-fold for AC-K, VSTN, ISTN, DRN, and DEET due to the substantially larger consumption of O_3 verified in 55 s (2.8 g m^{-3} – test #3 in Table 3).

3.1.2. *Estimation of ozone mass transfer rate and kinetic regime*

The kinetics regime of O_3 reactions are predominantly governed by absorption theories in gas-liquid reactions [18,73]. According to the two-film theory, the mass transfer of O_3 from the gas phase to the liquid phase in the presence of chemical reactions is usually calculated by Eq. (8) [16]:

$$N_{O_3} = k_L a \times ([O_3^*] - [O_3]_L) \times E;\ with\ k_L = \frac{k_L a}{a} = \frac{D_{O_3}}{\delta} \quad (8)$$

where N_{O_3} is the O_3 mass transfer rate or absorption rate of O_3 (M s^{-1}); $k_L a$ is the product of the O_3-liquid mass transfer coefficient (k_L, in m s^{-1}) and the specific interfacial area (a, in m^2 m^{-3}); $[O_3^*]$ and $[O_3]_L$ are the dissolved O_3 concentration at the interface and in the bulk liquid (in M), respectively; and E is the enhancement factor, which captures the influence of the chemical reaction on the mass transfer at the gas-liquid interface. The value of k_L is related to the diffusion coefficient of O_3 in water (D_{O3} = 1.74 ×10^{-9} m^2 s^{-1} [74]) and the liquid film thickness (δ, in μm) surrounding the gas bubble. Fig. 4a illustrates the diffusion of O_3 from the gas phase into the SW matrix through the liquid film and the reactive CECs from the liquid bulk into the liquid film, according to the two-film theory.

As a consequence of adopting the two-film theory, it was possible to quantify the enhancement factor by determining if the oxidation reactions mainly occurred within the liquid film, or in the water bulk. Conditions representing the experiments performed in the NETmix reactor for an applied O_3 dose of 9 g m^{-3} (test #2, Table 3) were selected to estimate the O_3 absorption rate. The $[O_3]_G^{in}$ was set to 30 g m^{-3}. As Henry's law relates $[O_3]_G^{in}$ with $[O_3^*]$ by the dimensionless Henry constant (H), in which $H = \frac{[O_3^*]}{[O_3]_G^{in}}$, it is obtained $[O_3^*]$ = 7.2 g m^{-3} (or 1.5×10^{-4} M) for H = 0.24 [75]. Furthermore, the residual O_3 in the liquid was measured, $[O_3]_L$ = 2.9±0.1 g m^{-3} (or (6.0±0.2)×10^{-5} M), considering

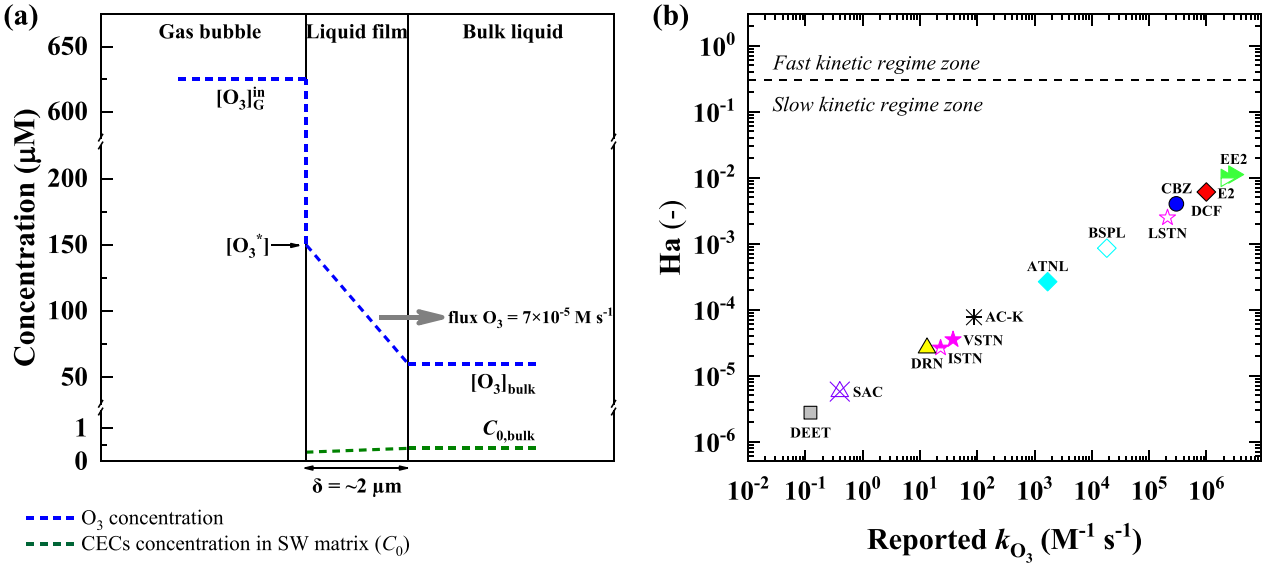

Fig. 4. (a) Qualitative scheme of O_3 and reactive CECs diffusion through the liquid film, according to the two-film theory. **(b)** Hatta number (*Ha*) of the direct reaction of O_3 with CECs with rate constants (k_{O3}) of these reactions. Conditions: *AOD* = 9 g m^{-3}; pH = 6.8; Q_L = 100 dm^3 h^{-1} and k_L = 1.1×10^{-3} m s^{-1} (test #2, see Table 3). Liquid film thickness (δ = ~2 μm) was calculated according to Eq. 8.

the steady-state reaction conditions.

As such, to evaluate whether the mass transfer was improved by the chemical reaction, an essential parameter is the Hatta number (*Ha*), which establishes a comparison between the chemical reaction phenomenon and the mass transfer rate. It is defined by Eq.(9) [18]:

$$Ha = \frac{\sqrt{k_{O_3} \times D_{O_3} \times C_0}}{k_L} \quad (9)$$

where k_{O3} is the rate constant of the direct reaction between O_3 and the contaminant (M^{-1} s^{-1}), and C_0 is the initial CECs concentration in the feed liquid stream (in M). According to the two-film theory, values of $E > 1$ and *Ha* between 0.3 and 3 designate the development of a fast reaction with the comparatively slower mass transfer becoming the main controlling step, while $E = 1$ and $Ha < 0.3$ mean chemical control of the reaction rate [1,18]. Moreover, it is important to highlight that the contaminant concentration and the reaction rate constant are the two factors that most significantly influence the *Ha,* indicating that the kinetic regimes of any O_3 reactions are independent of the water matrix in which the reactions occur [1].

In the present work, the necessary information to compute *Ha* was obtained for 13 of the 19 CECs spiked in SW from k_{O3} values available in literature (Table 3). For $Q_G = 30$ Ndm^3 h^{-1} and $Q_L = 100$ dm^3 h^{-1}, a k_L value of 1.1×10^{-3} m s^{-1} was calculated considering $k_La = 0.77$ s^{-1} and $a = 696$ m^2 m^{-3} obtained in Pituco et al. [33] and estimated by a CFD methodology [39], respectively. The calculated k_L surpasses those associated with venturi injectors and fine bubble diffusers coupled in a bubble tank or column, typically applied in WWTPs, by one to two orders of magnitude [33,73].

Fig. 4b shows *Ha* as a function of k_{O3} corresponding to the direct O_3 oxidation of 13 CECs that have been spiked in SW. Notably, the *Ha* values for these contaminants were observed to remain below 0.02. This means that all reactions between O_3 and CECs ($C_0 = 10$ μg L^{-1}) were chemically controlled at $k_L = 1.1\times10^{-3}$ m s^{-1}. According to Beltrán (2004) [18], this indicates that the reaction is very slow compared to the gas-liquid mass transfer phenomenon and exclusively occurs within the water bulk, i.e., the dissolved O_3 diffuses exceedingly quickly through the thin film layer (δ = ~2 μm) to attain the bulk liquid where it will react. In this scenario, the O_3 mass transfer was not accelerated by the reaction between the CECs and O_3 (Ha < 0.3 and $E = 1$), which implies that the rate of consumption of O_3 by the micropollutants was much lower than the mass transfer rate of O_3 from the gaseous to liquid phase ($N_{O3} = 7\times10^{-5}$ M s^{-1}). Therefore, the NETmix improves the reaction in the liquid bulk due to the larger k_L values with which it is associated.

3.2. Performance of the NETmix in the removal of CECs spiked in tertiary-treated urban wastewater effluent

3.2.1. Effect of gas-phase ozone concentration and gas flowrate

In a more realistic water contamination scenario, the performance of quaternary treatment using the NETmix reactor was firstly assessed for UWW1 spiked with 19 CECs (signaled with '†' in Table 1) by maintaining the applied O_3 dose at 18 g m^{-3} (1.15 g_{O_3} g_{DOC}^{-1}), while the $[O_3]_G^{in}$ was set at 40 and 60 g Nm^{-3} (test #5 and #6, Table 3). Q_L was fixed at 100 dm^3 h^{-1}, corresponding to the system's residence time of about 55 s. From the results shown in Fig. 5a, every tested condition led to ≥ 80% removal (or below the LOQ) for 5 of the 19 CECs. Nonetheless, it was observed an improvement in the CECs abatement due to an increase in the inlet gas-phase O_3 concentration. Fig. 5b shows the O_3 transfer yield obtained in the tests: while 63% of the supplied O_3 was successfully transferred into the water for $[O_3]_G^{in} = 40$ g Nm^{-3}, when it was applied $[O_3]_G^{in} = 60$ g Nm^{-3}, the O_3 transfer yield increased up to 71%, consequently favoring the CECs removal efficiency. This result can be justified by traditional mass transfer theories, in which, by increasing the gas-phase O_3 concentrations, a larger driving force can be obtained, favoring a larger diffusion rate of O_3, i.e., more O_3 from the gas phase is transferred to liquid phase [76]. Consequently, more O_3 is readily available to oxidize CECs. Moreover, to reach identical *AOD* values whilst maintaining similar hydrodynamic conditions and raising $[O_3]_G^{in}$, it was necessary to reduce the inlet Q_G from 45 to 30 Ndm^3 h^{-1}. For the NETmix reactor, it was verified that, for the same Q_L (100 dm^3 h^{-1}), the mass transfer efficiency increases with the reduction of Q_G, as it results in a larger gas-liquid contact time [33]. Therefore, although the same *AOD* was applied (1.15 g_{O_3} g_{DOC}^{-1}) by increasing the $[O_3]_G^{in}$, the *TOD* increased (0.81 *vs.* 0.71 g_{O_3} g_{DOC}^{-1}, Fig. 5b) due to a larger transfer yield.

3.2.2. Effect of ozone dose

Fig. 6 shows the effect of the O_3 dose on the abatement of 19 target CECs spiked in UWW1 and UWW2 matrices. For this, Q_L and Q_G were set at 100 dm^3 h^{-1} ($\tau_{system} = 55$ s) and 30 Ndm^3 h^{-1}, respectively, and $[O_3]_G^{in}$ was varied according to *AOD* (Table 3). As expected, a general tendency can be observed, in which increasing the O_3 doses enhanced the CECs removal efficiency. The CECs also exhibited several degrees of degradation, which may be attributed to the difference in reactivity between each contaminant and the oxidizing species. As seen by the wide range of second-order rate constant values associated with ozone (k_{O3}) and hydroxyl radicals ($k_{\bullet HO}$) displayed in Table 1, both oxidants vary significantly in their reactivity. O_3 in aqueous solution naturally decomposes by reaction with hydroxide ion (OH^-) followed by formation

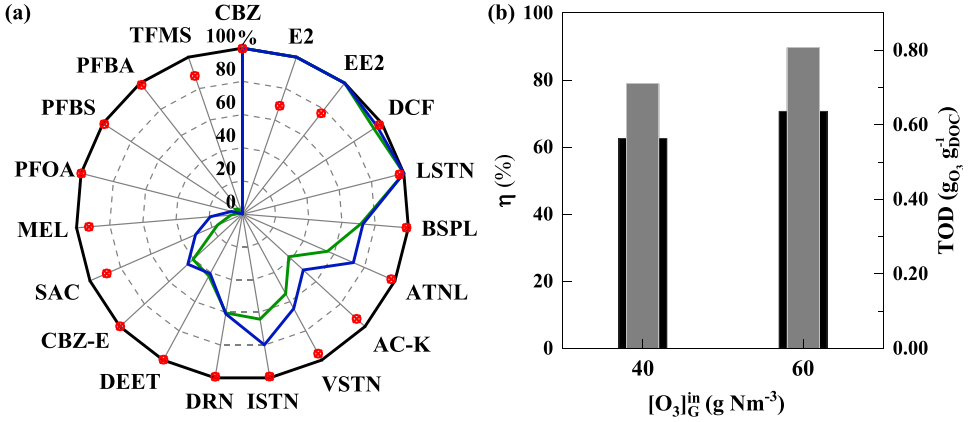

Fig. 5. **(a)** Removal of CECs ($C_0 = 10$ μg dm^{-3}) at ozone concentrations in the gas-phase inlet of 40 (; test #5) and 60 (; test #6) g Nm^{-3}. **(b)** Ozone transfer yield (% –) and transferred ozone dose (g_{O_3} g_{DOC}^{-1} –) employed. The red symbol () indicates the limit of quantification (LOQ) of the method. Conditions: see Table 3.

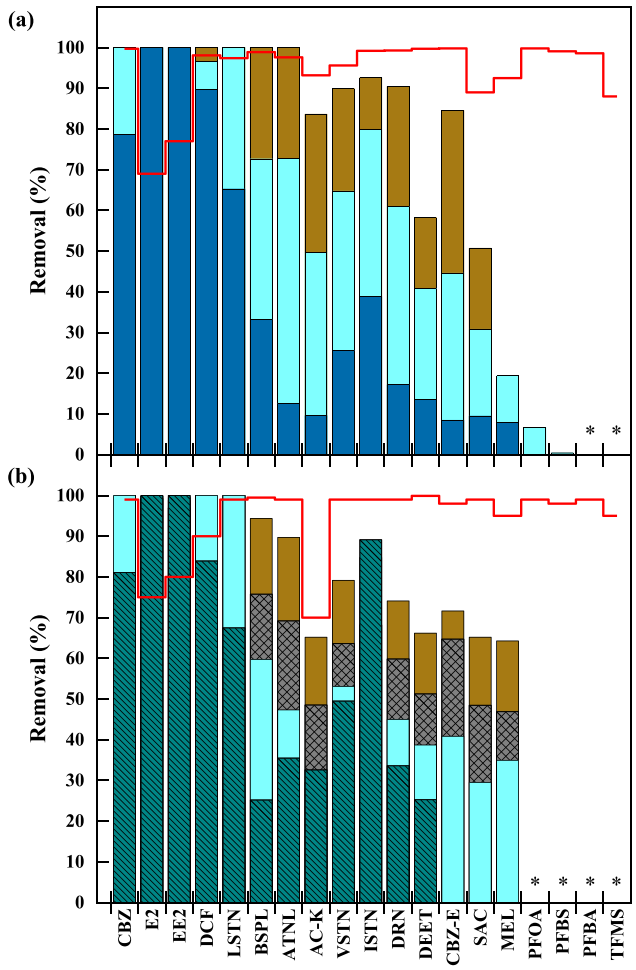

Fig. 6. Removal efficiency (%) related to the 19 CECs spiked in **(a)** UWW1 and **(b)** UWW2 ($C_0 = 10$ μg dm^{-3}) after 55 s contact time under the following doses: AOD = 0.57 (– test #4), 0.9 (– test #8), 1.15 (– test #5; #9), 1.5 (– test #10) and 2.0 (– test #7; #11) g_{O_3} g_{DOC}^{-1}. The red lines indicate the limit of quantification (LOQ) of the method. * No removal.

of free radical •OH. On the one hand, O_3 attacks selectively specific functional groups, while, on the other hand, •OH reacts quickly and unselectively with a large set of molecules [17,19].

For simplicity, CECs were classified into three groups as a function of the respective reported k_{O3} [77,78]: (i) O_3-reactive ($k_{O3} \geq 10^4$ M^{-1} s^{-1}), (ii) O_3 moderately-reactive (10^2 M^{-1} s^{-1} $\leq k_{O3} < 10^4$ M^{-1} s^{-1}), and (iii) O_3 resistant ($k_{O3} < 10^2$ M^{-1} s^{-1}). Analogously, a method for a more accurate abatement prediction can be given by a further sub-division into two categories based on $k_{\bullet OH}$: low-to-intermediate reactivity contaminants when $k_{\bullet OH} < 5\times10^9$ M^{-1} s^{-1} and high reactivity contaminants when $k_{\bullet OH} \geq 5\times10^9$ M^{-1} s^{-1} [58,77].

As such, the ozonation showed satisfactory degradation (≥80% or below LOQ) for micropollutants most readily reactive with O_3 ($k_{O3} \geq 10^4$ M^{-1} s^{-1}) such as CBZ, E2, EE2, DCF (and LSTN with removal >65%), applying an O_3 dose of 0.57 g_{O_3} g_{DOC}^{-1} (*TOD* = 0.43 g_{O_3} g_{DOC}^{-1}) for UWW1 and 0.9 g_{O_3} g_{DOC}^{-1} (*TOD* = 0.27 g_{O_3} g_{DOC}^{-1}) for UWW2. This finding suggests that O_3-reactive contaminants are prone to sufficient degradation via direct oxidations with O_3 at even lower O_3 doses, which agrees with observations commonly found in the literature [5,15,46]. These contaminants have functional groups that are strongly reactive with O_3, such as olefins (e.g., CBZ), phenol (e.g., E2, EE2), aniline (e.g., DCF) and benzene rings (e.g., CBZ, LSTN) [14,51,60]. Contrastingly, contaminants with $k_{O3} < 10^4$ M^{-1} s^{-1} were favorably removed by increasing *AOD*. A relatively intermediate O_3 dose of 1.15 g_{O_3} g_{DOC}^{-1} (*TOD* of 0.81 and 0.35 g_{O_3} g_{DOC}^{-1} for UWW1 and UWW2, respectively) and 1.50 g_{O_3} g_{DOC}^{-1} (*TOD* = 0.54 g_{O_3} g_{DOC}^{-1} for UWW2) were applied and led to good removal performance levels between 50% and 80% to O_3-moderately-reactive contaminants (BSPL and ATNL). Furthermore, good removal efficiencies (58 – 92%) were also observed for contaminants with high O_3 resistance ($k_{O3} < 10^2$ M^{-1} s^{-1}), as AC-K, VSTN, ISTN, DRN, DEET, CBZ-E and SAC, when it was utilized the largest O_3 doses of 2.0 g_{O_3} g_{DOC}^{-1} for both wastewater matrices (*TOD* equivalent to 1.28 and 0.76 g_{O_3} g_{DOC}^{-1} for UWW1 and UWW2, respectively). The only CECs that persisted without significant degradation (<10%), even when subjected to the largest O_3 dose, were the perfluoroalkyl substances – PFAS (PFBA, PFOA, PFBS, and TFMS). These organic contaminants contain carbon-fluorine bonds that render them exceedingly stable and resistant to the attack of O_3 and the •OH radical [17].

In general, during O_3 exposure, both O_3 and •OH reached sufficient concentration levels to effectively degrade the contaminants. Fig. 7 shows that CECs removal was strongly correlated with reported k_{O3} and $k_{\bullet OH}$ (data shown for UWW2 at *AOD* = 2.0 g_{O_3} g_{DOC}^{-1} and *TOD* = 0.76 g_{O_3} g_{DOC}^{-1}). As the O_3 rate constant increases, an enhancement in removal is observed (Fig. 7a). For contaminants with low k_{O3}, the extent of degradation was more significantly related to $k_{\bullet OH}$ rather than k_{O3} (Fig. 7b). This suggests that the substantial abatement for O_3-resistant contaminants was mainly driven by unselective oxidant •OH exposure formed from O_3-decomposition in the alkaline pH (around 7.3) of the UWW matrix [58]. It should be noted that, for the two UWW matrices, the removal efficiency of O_3-resistant contaminants generally increased proportionally to their $k_{\bullet OH}$ (ISTN > VSTN > DRN > DEET > AC-K > SAC – highlighted region in light blue in Fig. 7b for UWW2).

3.2.3. *Effect of the UWW matrix*

As indicated in the comparison between the obtained removal efficiencies for the tests with UWW1 and UWW2 provided in Fig. 6, apart from O_3-reactive CECs ($k_{O3} \geq 10^4$ M^{-1} s^{-1}, Table 1), which were associated with concentrations below the LOQ for both wastewaters, the removal of target CECs for UWW2 (MBR effluent – Fig. 6b) was globally unfavored for O_3-moderately-reactive and O_3-resistant contaminants (particularly for *AOD* of 1.15 and 2.00 g_{O_3} g_{DOC}^{-1}), most likely due to the presence of nitrite. Nitrite consumes O_3 quickly according to 1:1 stoichiometry: $NO_2^- + O_3 \rightarrow NO_3^- + O_2$, $k_{O3} = 3.7\times10^5$ M^{-1} s^{-1} [79]. For the UWW2 matrix, the nitrite concentration was 1.57 g N m^{-3}, which consumed 112 μM of O_3 – equivalent to 0.54 g_{O_3} g_{DOC}^{-1}. Thus, although the operating conditions were similar to those applied for UWW1, there was a significant reduction in *TOD* for the treatments with UWW2, influencing the removal of the CECs. The *TOD* for UWW2 ranged from 0.27 to 0.76 g_{O_3} g_{DOC}^{-1}, in contrast to the range of 0.43–1.28 g_{O_3} g_{DOC}^{-1} for UWW1, based on the ozone demand for nitrite oxidation according to: $g_{O_3}\ g_{DOC}^{-1} = g_{O_3}/g_{DOC} - 3.43 \times g_{NO_2\text{-}N}/g_{DOC}$ [80]. Typically, the specific O_3 doses applied in laboratory, pilot, and full scale ozonation studies are between 0.10 and 1.80 g_{O_3} g_{DOC}^{-1} [58,81,82], which is in the range of doses used for both UWW matrices tested in this work.

In addition to removing CECs, certain physicochemical characteristics of UWW1 and UWW2 exhibited enhancements due to the O_3 treatment. In Table 2, it is compared the parameters resulting from tests #7 and #11 (see Table 3). DOC was reduced by 8% and 3%, COD by 17% and 39%, TSS by 69% and 59%, and UVA_{254} by 48% and 43% for UWW1 (*TOD* = 1.28 g_{O_3} g_{DOC}^{-1}) and UWW2 (*TOD* = 0.74 g_{O_3} g_{DOC}^{-1}), respectively. These findings indicate that dissolved organic matter was the predominant consumer of O_3 in the wastewater tested (e.g., unsaturated compounds and aromatic substances [83]). Nevertheless, the UWW chemical composition greatly affects the effectiveness of ozonation in removing dissolved organic matter and altering chemical structures

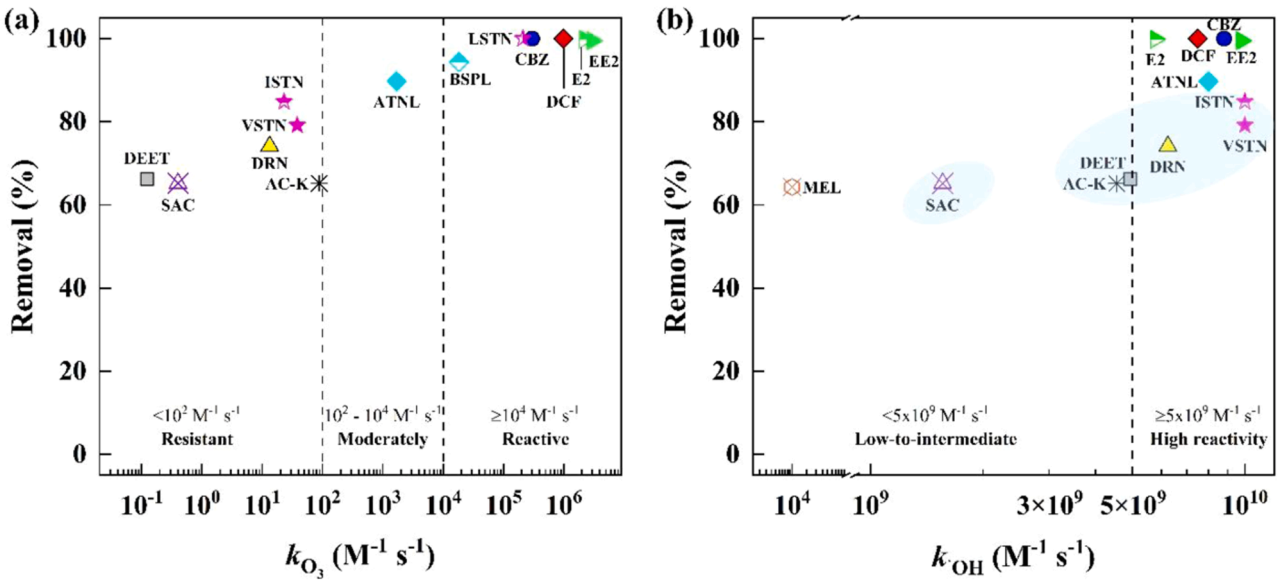

Fig. 7. Removal of CECs for *AOD* of 2.0 g_{O_3} g_{DOC}^{-1} (*TOD* = 0.76 g_{O_3} g_{DOC}^{-1}) as a function of **(a)** O_3 kinetic rate constants. CBZ-E, MEL, and PFAS were not included (k_{O3} unknown); and (b) reported •HO radical kinetic constants (highlighted region in light blue indicates O_3-resistant contaminants, $k_{O3} < 10^2$ M^{-1} s^{-1}). Data shown for UWW2. Conditions: test#11 – Table 3. The kinetic constant of target CECs is provided in Table 1.

[84]. Furthermore, the small reduction of DOC suggested that the performed ozonation reactions did not enable complete oxidation of bulk organic matter [77,85], similar to previous studies [5,15,77], which obtained a DOC reduction of 5–30% when applying 0.65–0.70 g_{O_3} g_{DOC}^{-1}.

Among the selected inorganic compounds analyzed (Table 2), most had concentrations similar to those found before the ozonation treatment. For UWW1, it was observed that ozonation led to an increase in nitrate concentration (Table 2), mainly due to ammonia oxidation. Previous studies have shown that this process is likely driven by the direct reaction with molecular O_3 ($NH_3 + 4O_3 \rightarrow NO_3^- + 4O_2 + H_3O^+$; $k_{O3} = 20$ M^{-1} s^{-1} [86]) [15,87,88]. Parallelly, the pronounced decrease in the ammonia concentration can also be associated with the indirect reaction with •OH ($NH_3 + {}^{\bullet}OH \rightarrow {}^{\bullet}NH_2 + H_2O$; $k_{\bullet OH} = 9.7 \times 10^7$ M^{-1} s^{-1} [89]) [17,24]. Moreover, the decrease in NH_4^+ can be partially related to ammonia stripping due to the ozone gas bubbling effect.

3.3. CECs measured in a screening campaign

3.3.1. Occurrence and post-treatment removal efficiencies of CECs

A total of 19 CECs were analyzed and detected in the raw wastewater (Table S3 - Supplementary Material). Their concentration levels ranged from 0.02 to 66.8 μg dm^{-3}, whereas the sum of all detected contaminants reached a total of 161 μg dm^{-3}. Among the substances detected, there were 12 pharmaceuticals (AMT, ASPD, ATNL, CBZ, FLE, ISTN, LAM, MET, SPD, TRA, TPD, and VEN); 1 drug metabolite (ODV); 3 pesticides (DRN, TBT, and DEET); 2 food additives (AC-K and CAFF); and 1 industrial chemical (TCPP) (Table 1). The CECs that presented the largest concentrations were the antidiabetic, MET – 66.8 μg dm^{-3}, the artificial sweetener, AC-K – 58.3 μg dm^{-3}, and the stimulant, CAFF – 19.0 μg dm^{-3}, followed by the antihypertensive, ISTN – 6.61 μg dm^{-3}, the drug metabolite, ODV – 3.25 μg dm^{-3}, and the industrial chemical, TCPP – 1.60 μg dm^{-3}. On the other hand, for the remaining contaminants, the detected concentrations were <1.00 μg dm^{-3}. A similar range of concentrations has been reported in other WWTPs located in Portugal and Galicia [5]. Regarding the wastewater treated by $WWTP_{II}$ (subjected to primary and secondary/tertiary treatments with activated sludge, followed by UV disinfection step), it is possible to verify in Table S3 that most CECs were associated with removal efficiency values lower than 40% (AMT, ASPD, ATNL, CBZ, FLE, ISTN, LAM, VEN, and DEET). TRA, TPD, ODV and DRN were the most persistent micropollutants presenting removal values between 0% and 10%. Only MET, AC-K and CAFF were removed >90% (although concentrations in the treated effluent were still as large as 6.16 and 0.27 μg dm^{-3} for MET and AC-K, respectively).

Similar removal efficiencies were found for 18 out of the 19 CECs analyzed in the MBR system (UWW2 matrix), in which the compounds most vulnerable to this treatment process were ISTN (56% removal efficiency), DRN (40%), TPD (32%), and VEN (31%). Furthermore, in addition to the 19 CECs analyzed in the post-MBR treatment wastewater, 13 supplementary CECs were assessed, resulting in an evaluation of 32 CECs, as shown in Table S3. Of these 32 targets, only the 25 CECs displayed in Fig. 8 were detected. This analysis showed that, despite the biological treatment, outlet concentrations were still significant, ranging from 0.04 to 8.40 μg dm^{-3}. The CECs with the largest outlet concentrations were the artificial sweetener, SAC – 8.4 μg dm^{-3}, and the flame retardant, MEL – 5.8 μg dm^{-3}, followed by two pharmaceuticals: the antihypertensive, ISTN – 3.6 μg dm^{-3}, and the anti-inflammatory, DCF –

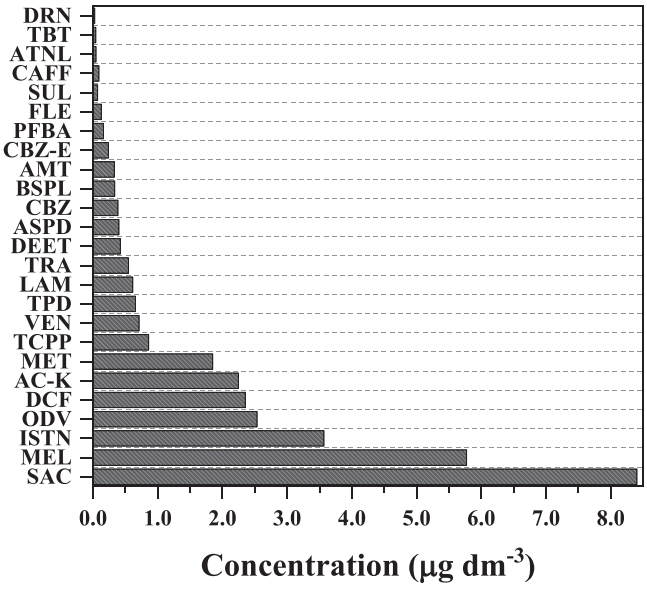

Fig. 8. Concentration of 25 CECs detected in the post-MBR treatment (UWW2).

2.3 μg dm^{-3}.

In general, the large concentration of artificial sweeteners (SAC and AC-K) could be correlated to its widespread use as sugar substitutes in sanitary products, foods, and beverages [90]. MEL is extensively used in the chemical industry (e.g., epoxy resins as a nitrogenous flame retardant) and its extensive application inevitably results in its introduction into the environment [91–93]. Meanwhile, the pharmaceuticals ISTN and DCF are highly consumed in Portugal – for instance, ISTN was a best-seller pharmaceutical in Portugal, Greece, France, and Belgium in 2018; and DCF already held the highest share in the Portuguese over-the-counter drugs market [94,95].

Overall, the results obtained in this work are consistent with previous findings reported in tertiary effluents from European WWTPs. For instance, SAC and AC-K concentrations have been measured up to 18 and 32 μg dm^{-3}, respectively [90,96,97], while the pharmaceuticals ISTN and DCF have been reported with average concentrations of up to 1.6 and 1.3 μg dm^{-3}, respectively [4,98]. It is important to highlight that, as indicated in the new revised European Directive concerning UWW treatment (Annex I) [7], state members must monitor the presence of ISTN and DCF (along with ASPD, CBZ, and VEN, which were also detected in this work) in wastewater in the coming years; and a removal efficiency by WWTPs of at least 80% for these substances is required [7].

3.3.2. Performance of ozonation process on CECs removal

The efficiency of the ozonation process performed by the NETmix reactor for the abatement of the 25 CECs detected in UWW2 was assessed under several *AOD* of 0.9, 1.15, 1.5 and 2.0 g_{O_3} g_{DOC}^{-1} (*TOD* ranged from 0.23 to 0.6 g_{O_3} g_{DOC}^{-1} – considering the ozone demand exerted by nitrite, as indicated by the procedure described in Section 3.2.3), resulting in the operating conditions for tests #12 to #15 of Table 3. As depicted in Fig. 9, increasing the O_3 doses led to a larger removal of CECs.

At the lowest ozone dose of 0.9 g_{O_3} g_{DOC}^{-1} (*TOD* = 0.23 g_{O_3} g_{DOC}^{-1}), 11 CECs were associated with ≥ 80% removal efficiency or beyond the LOQ, followed by the intermediate O_3 dose of 1.15 g_{O_3} g_{DOC}^{-1} (*TOD* = 0.3 g_{O_3} g_{DOC}^{-1}) with 19 CECs ≥80% (or beyond the LOQ) removal. The high removal rate can be associated with the rapid and complete consumption of O_3 by the CECs and dissolved organic matter, indicating that all *TOD* was below the immediate ozone demand *(IOD)* (see Chapter S2 of the Supplementary Material). Of these CECs, seven are highly reactive with O_3, with $k_{O3} \geq 10^4$ M^{-1} s^{-1}: DCF, CBZ, ASPD, SPD, FLE, BSPL, and ODV. These compounds contain electron-rich moieties such as amines, anilines, olefins, or phenols, which favorably react with O_3, as indicated in Table S4 [14,58].

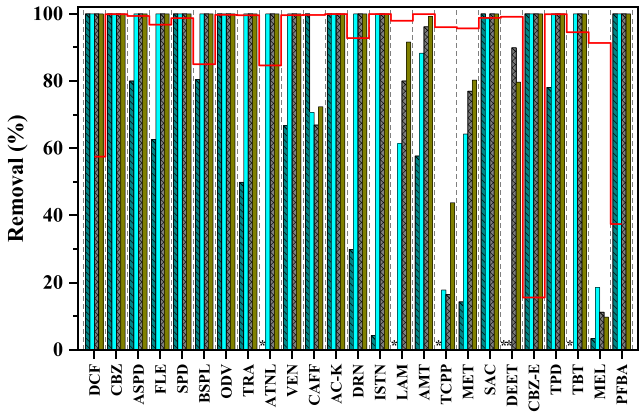

Fig. 9. Removal efficiency for the 25 target CECs detected in the UWW2, using the NETmix coupled with a contact column, operated in continuous mode (55 s) as function of applied ozone doses: 0.90 (– test #12), 1.15 (– test #13), 1.50 (– test #14) and 2.00 (– test #15) g_{O_3} g_{DOC}^{-1}. The red line indicates the limit of quantification (LOQ) of the method. * No removal.

In contrast, substances with lower O_3 but high •OH reactivity, such as AC-K, DRN, ISTN, and AMT, showed satisfactory abatement (to over 90%) at the lowest transferred O_3 dose (0.23 g_{O_3} g_{DOC}^{-1}), due to reaction with the strong and unselective oxidant •OH originated from the slightly alkaline pH (7.6±0.1) of the wastewater. In addition to the discussed in Section 3.2.2, indirect oxidation of contaminants with •OH is more influenced by the quality of the wastewater (e.g., the exposure of radical scavengers) than direct O_3 oxidation [99], which could explain the high abatement variation obtained for micropollutants with low O_3 reactivity. Hence, some contaminants, such as SAC and CBZ-E, also showed satisfactory removal, despite the low-to-intermediate •OH reactivity. Concerning PFBA, its large removal efficiency (>90%) was unexpected given its low O_3 reactivity due to its strong carbon-fluorine bonds. The very low PFBA concentration in UWW2 (0.16 μg dm^{-3}), close to the LOQ, led to significant analytical uncertainties and may explain the observed divergence.

Under the *AOD* between 1.15 and 2.0 g_{O_3} g_{DOC}^{-1} (*TOD* from 0.3 to 0.6 g_{O_3} g_{DOC}^{-1}), contaminants with low (or unknown) reactivity to O_3 and low reactivity to •OH exhibited improved removal as the O_3 dose increased. This improvement was observed for substances like LAM (61–92%), ATDN (67–88%), MET (64–80%), DEET (0–90%), TCPP (18–44%), and MEL (10–19%). In general, the increase in removal efficiency can be attributed to a larger exposure to •OH, resulting from the larger O_3 doses [100]. Furthermore, the competition between radical scavengers (e.g., bicarbonates/carbonates) and CECs for the available •OH, which naturally decreases the degradation kinetics of the targeted contaminants, is mitigated when larger O_3 doses are applied [101].

Overall, a maximum *AOD* of 2.0 g_{O_3} g_{DOC}^{-1} (corresponding to *TOD* of 0.6 g_{O_3} g_{DOC}^{-1}) resulted in removal values ≥80% for 22 out of the 25 CECs detected in the effluent from the MBR, at a very short HRT of 55 s. When compared to conventional O_3-in-water dispersion reactors, the CECs removal efficiencies achieved in this work occurred at a significantly shorter HRT (55 s) than the typical 5 – 30 min reported in lab, pilot, and full-scales ozonation process [21,22,78,81]. Using a reaction column with bubble diffuser to treat 21 CECs, Guillossou et al. [102] obtained an average removal ≥ 80% with an O_3 dose of 0.6 g_{O_3} g_{DOC}^{-1} and HRT of 10 min. Of the 21 compounds, 13 highly O_3-reactive micropollutants achieved ≥ 80% removal with an O_3 dose of 0.3 g_{O_3} g_{DOC}^{-1}, while >0.8 g_{O_3} g_{DOC}^{-1} was needed for less reactive compounds. In addition, the main characteristic of obtaining ≥80% removal values for a large quantity of CECs at exceedingly short contact times remains even when the proposed system is compared to alternative contacting systems. Prada-Vásquez et al.[5] used an O_3 membrane contactor with *TOD* up to 0.69 g_{O_3} g_{DOC}^{-1} and HRT of 60 s to achieve removals ≥80% for up to 12 out of 23 CECs detected in a secondary-treated wastewater effluent. Ekblad et al. [13], using a static mixer, reported removals ≥80% (or bellow LOQ) for up to 11 out of 20 CECs detected in a secondary-treated wastewater effluent, employing *TOD* of 0.8 g_{O_3} g_{DOC}^{-1} and HRT of 7 min in the contact tank. They also found no significant differences in the removal efficiency of 10 micropollutants when comparing to a typical static mixer and a venturi, achieving 60–80% removal for 4 CECs out of 11 CECs analysed (*TOD* = 0.4 g_{O_3} g_{DOC}^{-1} and HRT = 7 min) [13].

As seen from the results shown in Section 3.3.1, the tertiary treatment using a MBR presented a poor performance in CECs removal, corroborating with the fact that biological treatment systems usually are ineffective for these target compounds, requiring additional treatment steps [58,100,103]. Fig. 10 shows that, from the 19 target CECs detected in the raw wastewater (influent sample from $WWTP_{II}$), only CAFF, AC-K and MET were removed above 90%, considering primary, secondary (biological activated sludge) and tertiary treatment (MBR). The ozonation process (*TOD* = 0.6 g_{O_3} g_{DOC}^{-1}), implemented as quaternary

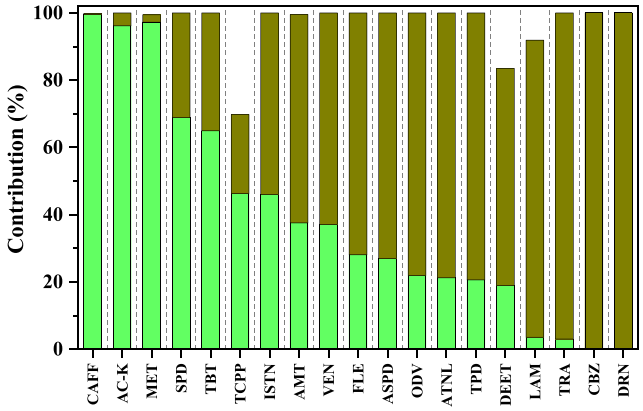

Fig. 10. Relative contribution (%) of primary/secondary/tertiary (MBR) ( ) system and ozonation process (; *TOD* = 0.6 g_{O_3} g_{DOC}^{-1} and HRT = 55 s – test #15) to the overall elimination of CECs detected in the raw wastewater (influent sample of $WWTP_{II}$).

treatment, was able to achieve removal values >80% for 18 out of 19 CECs detected (Fig. 10).

3.3.3. *Ozone post-treatment efficiencies on physicochemical parameters*

The efficiencies of O_3 post-treatment of UWW2 (without spiked CECs) were also investigated by assessing the removal of DOC, turbidity, and UVA_{254} as potential control parameters. Fig. 11 exhibits the removal of these parameters in relation to *TOD*.

As depicted in Fig. 11a, ozonation was minimally effective in removing DOC (up to 30%) and exhibited little variation across the different *TOD*. In the case of turbidity (Fig. 11b), an increase in its removal of 45–76% was achieved when *TOD* was raised from 0.23 to 0.60 g_{O_3} g_{DOC}^{-1}. Thus, O_3 can destroy solid particles of organic matter, even when low doses of O_3 are transferred [104,105].

The UVA_{254} is frequently used as a surrogate parameter for monitoring water quality. O_3 reacts very quickly with electron rich groups and decomposes carbon double bonds as well as aromatic rings, both of which are present in dissolved organic matter and are able to absorb electromagnetic radiation with wavelength at 254 nm [17,104,106]. Furthermore, the presence of aromatic substances, highly prevalent among CECs, is also well represented by UVA_{254}. As shown in Fig. 11c, a sustained decrease in the UVA_{254} absorption (42%) was reached with a

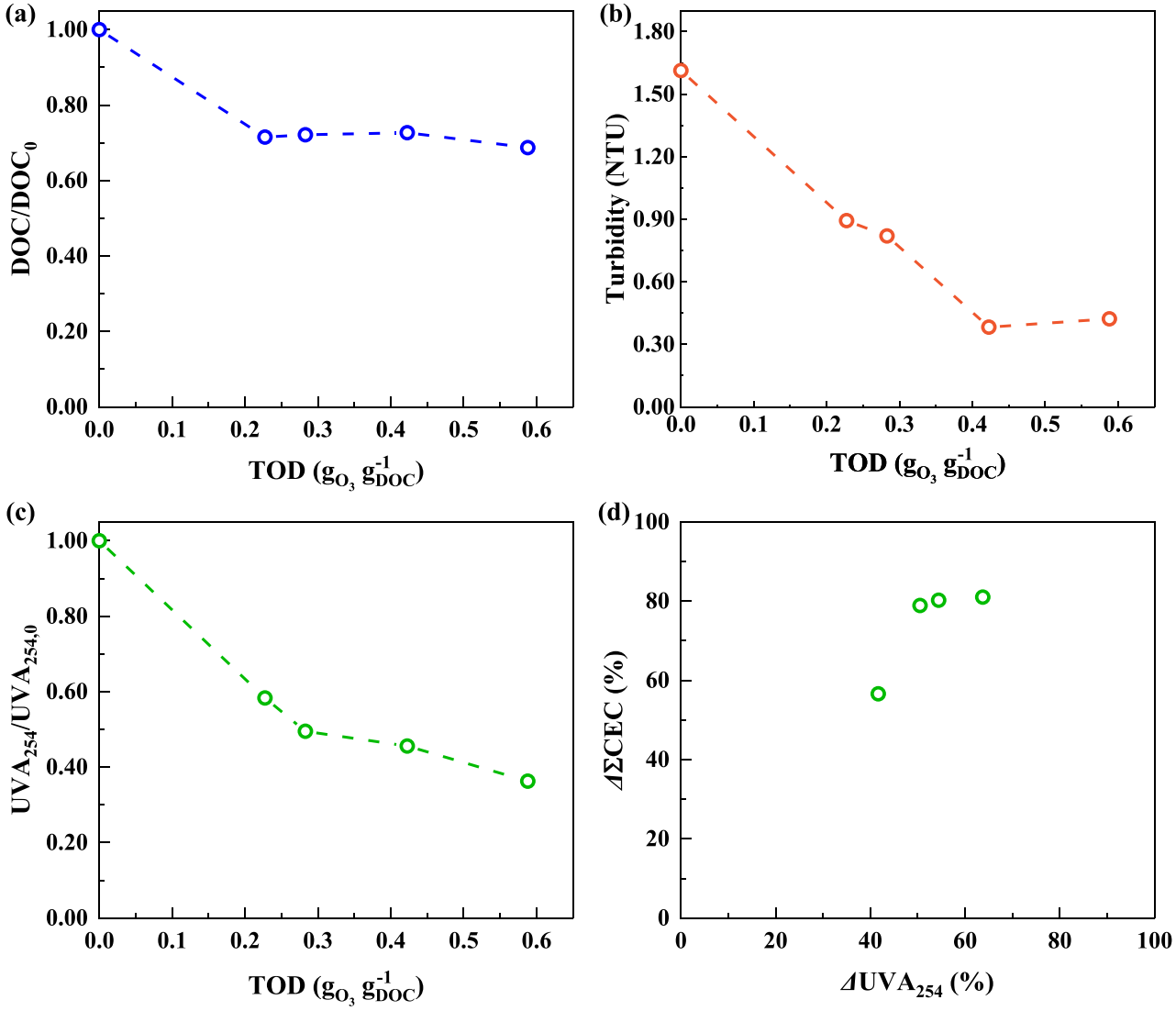

Fig. 11. (a) DOC/DOC_0 versus *TOD*; (b) Turbidity evolution versus *TOD*; **(c)** $UVA_{254}/UVA_{254,0}$ versus *TOD*; and **(d)** correlation between CECs removal and UVA_{254} reduction.

TOD of 0.23 g_{O_3} g_{DOC}^{-1}, while a larger decrease (64%) was achieved for an O_3 dose of 0.60 g_{O_3} g_{DOC}^{-1}. As such, a first-order kinetic relationship between the decay of UVA_{254} and O_3 exposure (in terms of *TOD*, in M) could be established: – $ln(UVA_{254}/UVA_{254,0}) = k_{UVA254} \times TOD$, where k_{UVA254} (in M^{-1}) is the rate of UVA_{254} reduction along the ozonation process [82]. A value of k_{UVA254} as large as $(4.0\pm0.2)\times10^3$ M^{-1} (R^2 = 0.992) was exhibited for the UWW2 matrix (without spiked CECs). This can be useful to improve the monitoring of ozonation processes in order to satisfy their specific treatment requirements [5]. Fig. 11d shows the relationship between the percentage of the total CECs elimination ($\Delta\sum$CECs) plotted as a function of a variation of the UVA_{254}. At small *TOD* (0.23 g_{O_3} g_{DOC}^{-1}), there is a smaller ΔUVA_{254}, leading to a small $\Delta\sum$CECs, as the applied O_3 is instantaneously consumed by the reactive compounds of the UWW2 matrix. However, by increasing the O_3 dose, once the *IOD* has been achieved, more residual dissolved O_3 was available in the liquid (Figure S2) and more $^{\bullet}OH$ could be formed via O_3 decomposition. Consequently, ΔUVA_{254} removal was substantially improved. About 80% of CECs were removed at 50–64% of ΔUVA_{254}, showing that the ozone dosages could remove aromatic compounds from the wastewater matrix.

4. Conclusions

The present study demonstrated, for the first time, the application of the NETmix static mixer as an O_3 gas injection system to promote the quaternary treatment of UWW. The NETmix network takes advantage of the successive contacting and splitting of flows to boost mass transfer rates and rapidly develop an O_3-rich stream to react with CECs. An applied O_3 dose of 9 g m^{-3} was enough to achieve a satisfactory degradation (≥80% or below the LOQ) for 8 out of 19 target CECs for experiments performed with demineralized water and considering only the nearly-zero contact time (0.61 s) in the NETmix reactor. Moreover, improvements in CECs removal efficiency were evidenced when a contact column was attached to the NETmix reactor to increase the residence time (55 s), showing 1.1–1.5-fold larger removal efficiencies for at least five target CECs.

In a more realistic wastewater contamination scenario, tests were performed to evaluate the effect of the applied (0.57–2.0 g_{O_3} g_{DOC}^{-1}) O_3 doses (corresponding to 0.23–1.28 g_{O_3} g_{DOC}^{-1} transferred O_3 doses) on the abatement of 19 target CECs spiked in two UWW matrices (UWW1, from a secondary settler tank; and UWW2, from a MBR treatment outlet). A general trend could be seen whereby CEC removal efficiency increases with increasing O_3 dosage. A maximum applied O_3 dose of 2.0 g_{O_3} g_{DOC}^{-1} (corresponding to a *TOD* of 1.28 and 0.76 g_{O_3} g_{DOC}^{-1} for UWW1 and UWW2, respectively) and system residence time of 55 s resulted in the removal values above 80% for 11 out of 19 spiked CECs in UWW1, and 9 out of 19 spiked CECs in UWW2. Moreover, the quality of the two UWW matrices - coming from different biological treatments - affected the ozonation treatment efficiency, highlighting the relevance of analyzing the organic/inorganic load of the effluent to adequately adjust the specific applied O_3 dose.

Additionally, the NETmix was also applied to eliminate 25 CECs detected in a screening campaign performed on the post-MBR treatment wastewater sample. The ozonation process proved to be very effective in the removal of 22 out of 25 CECs, with a maximum specific O_3 dose of 0.6 g_{O_3} g_{DOC}^{-1}. In general, the removal of CECs was strongly correlated with the ozone and hydroxyl radical reaction affinities, resulting in characteristic degradation patterns according to groups based on the respective kinetics rate constants. These achievements demonstrated the significant potential of the NETmix technology as an attractive alternative for O_3-driven wastewater treatment. In addition, future studies could further demonstrate a proper understanding of the cost and life cycle assessment associated with the NETmix reactor in order to ensure a sustainable and long-term operation of this technology.

CRediT authorship contribution statement

Mateus Mestriner Pituco: Writing – original draft, Methodology, Investigation, Formal analysis, Data curation. **Paulo H. Marrocos:** Writing – original draft, Validation, Methodology, Formal analysis. **Sandra Méndez:** Writing – review & editing, Methodology, Investigation, Data curation. **Rosa Montes:** Writing – review & editing, Validation, Supervision, Methodology, Investigation. **Rosario Rodil:** Writing – review & editing, Validation, Supervision, Resources, Methodology. **Francisca C. Moreira:** Writing – review & editing, Validation, Supervision, Methodology. **Vítor J.P. Vilar:** Writing – review & editing, Validation, Supervision, Resources, Project administration, Funding acquisition, Conceptualization.

Declaration of Competing Interest

The authors declare that they have no known competing financial interests or personal relationships that could have appeared to influence the work reported in this paper.

Acknowledgments

This work was supported by national funds through FCT/MCTES (PIDDAC): Project PTDC/EAM-AMB/4702/2020 - Cutting-Edge Ozone-Technology for Water, with DOI 10.54499/PTDC/EAM-AMB/4702/2020 (https://doi.org/10.54499/PTDC/EAM-AMB/4702/2020); LSRE-LCM, UIDB/50020/2020 (DOI: 10.54499/UIDB/50020/2020) and UIDP/50020/2020 (DOI: 10.54499/UIDP/50020/2020); and ALiCE, LA/P/0045/2020 (DOI: 10.54499/LA/P/0045/2020). M. M. Pituco and P.H. Marrocos acknowledge FCT for their Ph.D. scholarships (SFRH/BD/144673/2019 – DOI: 10.54499/SFRH/BD/144673/2019; and 2022.10437.BD, respectively). F. C. Moreira and V. J. P. Vilar acknowledge the FCT Individual Call to Scientific Employment Stimulus 2017 (CEECIND/02196/2017 and CEECIND/01317/2017, respectively). M.M. Pituco also gives special thanks to **Instituto Universitario de Investigación del Agua, Cambio Climático y Sostenibilidad (IACYS), Departamento de Ingeniería Química y Química Física – Universidad de Extremadura**, under the supervision of Prof. Dr. Eva M. Rodríguez, for the assistance with the procedure to determinate the absolute rate constants of ozone-saccharin reaction.

Appendix A. Supporting information

Supplementary data associated with this article can be found in the online version at doi:10.1016/j.jece.2025.115465.

Data availability

Data will be made available on request.

References

[1] F.J. Beltrán, A. Rey, Free radical and direct ozone reaction competition to remove priority and pharmaceutical water contaminants with single and hydrogen peroxide ozonation systems, Ozone.: Sci. Eng. 40 (2018) 251–265, https://doi.org/10.1080/01919512.2018.1431521.

[2] M.B. Ahmed, J.L. Zhou, H.H. Ngo, W. Guo, N.S. Thomaidis, J. Xu, Progress in the biological and chemical treatment technologies for emerging contaminant removal from wastewater: A critical review, J. Hazard. Mater. 323 (2017) 274–298, https://doi.org/10.1016/j.jhazmat.2016.04.045.

[3] L. Prieto-Rodríguez, I. Oller, N. Klamerth, A. Agüera, E.M. Rodríguez, S. Malato, Application of solar AOPs and ozonation for elimination of micropollutants in municipal wastewater treatment plant effluents, Water Res 47 (2013) 1521–1528, https://doi.org/10.1016/j.watres.2012.11.002.

[4] R. Montes, S. Méndez, J. Cobas, N. Carro, T. Neuparth, N. Alves, M.M. Santos, J. B. Quintana, R. Rodil, Occurrence of persistent and mobile chemicals and other contaminants of emerging concern in Spanish and Portuguese wastewater treatment plants, transnational river basins and coastal water, Sci. Total Environ. 885 (2023) 163737, https://doi.org/10.1016/j.scitotenv.2023.163737.

[5] M.A. Prada-Vásquez, M.M. Pituco, M.P. Caixeta, S.A. Cardona Gallo, A.M. Botero-Coy, F. Hernández, R.A. Torres-Palma, V.J.P. Vilar, Ozonation using a stainless-steel membrane contactor: Gas-liquid mass transfer and pharmaceuticals removal from secondary-treated municipal wastewater, Chemosphere 349 (2024) 140888, https://doi.org/10.1016/j.chemosphere.2023.140888.
[6] R. Montes, S. Méndez, N. Carro, J. Cobas, N. Alves, T. Neuparth, M.M. Santos, J. B. Quintana, R. Rodil, Screening of contaminants of emerging concern in surface water and wastewater effluents, assisted by the persistency-mobility-toxicity criteria, Molecules 27 (2022) 3915, https://doi.org/10.3390/molecules27123915.
[7] European Commission, Proposal for a revised Urban Wastewater Treatment Directive, https://Environment.Ec.Europa.Eu/Publications/Proposal-Revised-Urban-Wastewater-Treatment-Directive_en (2022).
[8] Y. Lee, U. von Gunten, Advances in predicting organic contaminant abatement during ozonation of municipal wastewater effluent: reaction kinetics, transformation products, and changes of biological effects, Environ. Sci.: Water Res. Technol. 2 (2016) 421–442, https://doi.org/10.1039/C6EW00025H.
[9] O.M. Rodriguez-Narvaez, J.M. Peralta-Hernandez, A. Goonetilleke, E.R. Bandala, Treatment technologies for emerging contaminants in water: A review, Chem. Eng. J. 323 (2017) 361–380, https://doi.org/10.1016/j.cej.2017.04.106.
[10] R.I.L. Eggen, J. Hollender, A. Joss, M. Schärer, C. Stamm, Reducing the discharge of micropollutants in the aquatic environment: the benefits of upgrading wastewater treatment plants, Environ. Sci. Technol. 48 (2014) 7683–7689, https://doi.org/10.1021/es500907n.
[11] S.G. Zimmermann, M. Wittenwiler, J. Hollender, M. Krauss, C. Ort, H. Siegrist, U. von Gunten, Kinetic assessment and modeling of an ozonation step for full-scale municipal wastewater treatment: micropollutant oxidation, by-product formation and disinfection, Water Res 45 (2011) 605–617, https://doi.org/10.1016/j.watres.2010.07.080.
[12] C.M. Morrison, S. Hogard, R. Pearce, A. Mohan, A.N. Pisarenko, E.R. V. Dickenson, U. von Gunten, E.C. Wert, Critical review on bromate formation during ozonation and control options for its minimization, Environ. Sci. Technol. 57 (2023) 18393–18409, https://doi.org/10.1021/acs.est.3c00538.
[13] M. Ekblad, R. Juárez, P. Falås, K. Bester, M. Hagman, M. Cimbritz, Influence of operational conditions and wastewater properties on the removal of organic micropollutants through ozonation, J. Environ. Manag. 286 (2021) 112205, https://doi.org/10.1016/j.jenvman.2021.112205.
[14] M. Bourgin, B. Beck, M. Boehler, E. Borowska, J. Fleiner, E. Salhi, R. Teichler, U. Von Gunten, H. Siegrist, C.S. Mcardell, Evaluation of a full-scale wastewater treatment plant upgraded with ozonation and biological post-treatments: Abatement of micropollutants, formation of transformation products and oxidation by-products, Water Res 129 (2018) 486–498, https://doi.org/10.1016/j.watres.2017.10.036.
[15] P.H. Presumido, S. Ribeirinho-Soares, R. Montes, J.B. Quintana, R. Rodil, M. Ribeiro, T. Neuparth, M.M. Santos, M. Feliciano, O.C. Nunes, A.I. Gomes, V.J. P. Vilar, Ozone membrane contactor for tertiary treatment of urban wastewater: Chemical, microbial and toxicological assessment, Sci. Total Environ. 892 (2023) 164492, https://doi.org/10.1016/j.scitotenv.2023.164492.
[16] C. Gottschalk, J.A. Libra, A. Saupe, Ozonation of water and waste water: A practical guide to understanding ozone and its applications, second ed., Wiley-VCH Verlag GmbH & Co. KGaA, Weinheim, 2010.
[17] C. von Sonntag, U. von Gunten, Chemistry of ozone in water and wastewater treatment: From basic principles to applications, first ed., IWA Publishing, London, 2012.
[18] F.J. Beltran, Ozone reaction kinetics for water and wastewater systems, first ed., CRC Press, London, 2004.
[19] T. Manasfi, Ozonation in drinking water treatment: an overview of general and practical aspects, mechanisms, kinetics, and byproduct formation, in: T. Manasfi, J.-L. Boudenne (Eds.), Comprehensive Analytical Chemistry, Elsevier, Amsterdam, 2021, pp. 85–116, https://doi.org/10.1016/bs.coac.2021.02.003.
[20] C. Tizaoui, O.O. Odejimi, A. Abdelaziz, Occurrence, effects, and treatment of endocrine-disrupting chemicals in Water, in: I.M. Mujtaba, R. Srinivasan, N. O. Elbashir (Eds.), The Water-Food-Energy Nexus: Processes, Technologies and Challenges, CRC Press, Boca Raton, 2017, pp. 157–179.
[21] K.F. Guerrero-Granados, J. Mante, M. Joy, M. Meier, A. Boergers, S. Panglisch, J. Tuerk, Ozone strong water dosing as optimized ozonation process for micropollutants reduction in wastewater treatment plants, Ozone.: Sci. Eng. (2024) 1–15, https://doi.org/10.1080/01919512.2024.2336973.
[22] K.L. Rakness, Ozone in drinking water treatment: Process design, operation, and optimization, first ed., American Water Works Association, Denver, 2005.
[23] P. Seridou, N. Kalogerakis, Disinfection applications of ozone micro- and nanobubbles, Environ. Sci. Nano 8 (2021) 3493–3510, https://doi.org/10.1039/D1EN00700A.
[24] B. Langlais, D. Reckhow, D. Brink, Ozone in Water Treatment - Application and Engineering, CRC Press, Boca Raton, 1991.
[25] T. Steinke, Sidestream injection shows its advantages in ozone systems, Int. Ozone Assoc. Ozone N. 49 (2021) 14–17.
[26] E.C. Wert, J. Lew, K.L. Rakness, Effect of ozone dissolution systems on ozone exposure and bromate formation, J. AWWA 109 (2017), https://doi.org/10.5942/jawwa.2017.109.0048.
[27] M.T. Gao, M. Hirata, H. Takanashi, T. Hano, Ozone mass transfer in a new gas-liquid contactor-Karman contactor, Sep. Purif. Technol. 42 (2005) 145–149, https://doi.org/10.1016/j.seppur.2004.07.004.
[28] A. Schmitt, J. Mendret, S. Brosillon, Evaluation of an ozone diffusion process using a hollow fiber membrane contactor, Chem. Eng. Res. Des. 177 (2022) 291–303, https://doi.org/10.1016/j.cherd.2021.11.002.
[29] H.P. Kaiser, O. Köster, M. Gresch, P.M.J. Périsset, P. Jäggi, E. Salhi, U. von Gunten, Process control for ozonation systems: a novel real-time approach, Ozone.: Sci. Eng. 35 (2013) 168–185, https://doi.org/10.1080/01919512.2013.772007.
[30] M.S. Baawain, M. Gamal El-Din, D.W. Smith, A. Mazzei, Hydrodynamic characterization and mass transfer analysis of an in-line multi-jets ozone contactor, Ozone.: Sci. Eng. 33 (2011) 449–462, https://doi.org/10.1080/01919512.2011.622705.
[31] A.K. Biń, Ozone dissolution in aqueous systems treatment of the experimental data, Exp. Therm. Fluid. Sci. 28 (2004) 395–405, https://doi.org/10.1016/j.expthermflusci.2003.03.001.
[32] A. Bin, M. Roustan, Mass transfer in ozone reactors, in: Fundamental and Engineering Concepts for Ozone Reactor Design, International Specialized Symposium IOA, Toulouse, France, 2000: pp. 99–131.
[33] M.M. Pituco, P.H. Marrocos, R.J. Santos, M.M. Dias, J.C.B. Lopes, F.C. Moreira, V. J.P. Vilar, NETmix technology as ozone gas injection system: Assessment of the gas-liquid mass transfer, Chem. Eng. Process.: Process. Intensif. (2023), https://doi.org/10.1016/j.cep.2023.109566.
[34] B. Lopes, P.E.M. dos S. da C. Laranjeira, M.M.G.Q. Dias, A.A.A. Martins, Network mixer and related mixing, in European Patent EP172643 B1. 2008, 2013, PCT/IB2005/000647, US Patent 8 434 933 B2., 2005.
[35] P.E. Laranjeira, A.A. Martins, J.C.B. Lopes, M.M. Dias, NETmix, a new type of static mixer: modeling, simulation, macromixing, and micromixing characterization, AICHE J. 55 (2009) 2226–2243, https://doi.org/10.1002/aic.11815.
[36] C.M. Fonte, M.E. Leblebici, M.M. Dias, J.C.B. Lopes, The NETmix reactor: Pressure drop measurements and 3D CFD modeling, Chem. Eng. Res. Des. 91 (2013) 2250–2258, https://doi.org/10.1016/j.cherd.2013.07.014.
[37] P.H. Marrocos, I.S. Fernandes, M.M. Pituco, J.C.B. Lopes, M.M. Dias, R.J. Santos, V.J.P. Vilar, CFD and lower order mechanistic models for gas-liquid flow in NETmix: Pressure drop and gas hold-up, Chem. Eng. Sci. 284 (2024) 119478, https://doi.org/10.1016/j.ces.2023.119478.
[38] J. Matos, R.J. Santos, M.M. Dias, J.C.B. Lopes, Mixing in the NETmix Reactor, Front. Chem. Eng. 3 (2021), https://doi.org/10.3389/fceng.2021.771476.
[39] I.S. Fernandes, M.S.C.A. Brito, Y.A. Manrique, M.M. Dias, J.C.B. Lopes, R. J. Santos, Experimental and numerical characterisation of two-phase flow in NETmix reactors, Chem. Eng. Process. 194 (2023) 109580, https://doi.org/10.1016/j.cep.2023.109580.
[40] M.J. Lima, C.G. Silva, A.M.T. Silva, J.C.B. Lopes, M.M. Dias, J.L. Faria, Homogeneous and heterogeneous photo-Fenton degradation of antibiotics using an innovative static mixer photoreactor, Chem. Eng. J. 310 (2017) 342–351, https://doi.org/10.1016/j.cej.2016.04.032.
[41] M.J. Lima, A.M.T. Silva, C.G. Silva, J.L. Faria, J.C.B. Lopes, M.M. Dias, An innovative static mixer photoreactor: Proof of concept, Chem. Eng. J. 287 (2016) 419–424, https://doi.org/10.1016/j.cej.2015.09.092.
[42] S.G.S. Santos, L.O. Paulista, B.A. Marinho, C. Passalía, M. Flores, M.D. Labas, R. J. Brandi, V.J.P. Vilar, A step forward on NETmix reactor for heterogeneous photocatalysis: Kinetic modeling of As(III) oxidation, Chem. Eng. J. 405 (2021), https://doi.org/10.1016/j.cej.2020.126612.
[43] S.G.S. Santos, L.O. Paulista, T.F.C.V. Silva, M.M. Dias, J.C.B. Lopes, R.A. R. Boaventura, V.J.P. Vilar, Intensifying heterogeneous TiO2 photocatalysis for bromate reduction using the NETmix photoreactor, Sci. Total Environ. 664 (2019) 805–816, https://doi.org/10.1016/j.scitotenv.2019.02.045.
[44] D.F.S. Morais, J.C.B. Lopes, M.M. Dias, V.J.P. Vilar, F.C. Moreira, eNETmix: A pioneering electrochemical flow reactor with enhanced mass transfer, Chem. Eng. J. 481 (2024) 148244, https://doi.org/10.1016/j.cej.2023.148244.
[45] V. Castro, J.B. Quintana, I. Carpinteiro, J. Cobas, N. Carro, R. Cela, R. Rodil, Combination of different chromatographic and sampling modes for high-resolution mass spectrometric screening of organic microcontaminants in water, Anal. Bioanal. Chem. 413 (2021) 5607–5618, https://doi.org/10.1007/s00216-021-03226-6.
[46] P.H. Presumido, R. Montes, J.B. Quintana, R. Rodil, M. Feliciano, G.L. Puma, A. I. Gomes, V.J.P. Vilar, Ozone membrane contactor to intensify gas/liquid mass transfer and contaminants of emerging concern oxidation, J. Environ. Chem. 10 (2022) 108671, https://doi.org/10.1016/j.jece.2022.108671.
[47] M. Mustafa, H. Wang, R.H. Lindberg, J. Fick, Y. Wang, M. Tysklind, Identification of resistant pharmaceuticals in ozonation using QSAR modeling and their fate in electro-peroxone process, Front. Environ. Sci. Eng. 15 (2021) 106, https://doi.org/10.1007/s11783-021-1394-6.
[48] J. An, G. Li, T. An, W. Song, H. Feng, Y. Lu, Photocatalytic degradation of three amantadine antiviral drugs as well as their eco-toxicity evolution, Catal. Today 258 (2015) 602–609, https://doi.org/10.1016/j.cattod.2015.01.004.
[49] J. Benner, E. Salhi, T. Ternes, U. von Gunten, Ozonation of reverse osmosis concentrate: Kinetics and efficiency of beta blocker oxidation, Water Res 42 (2008) 3003–3012, https://doi.org/10.1016/j.watres.2008.04.002.
[50] M. Mustafa, Removal of Micropollutants from Wastewater: evaluation of effect of upgrading ozonation to electro-peroxone, Umeå University, Department of Chemistry, 2020.
[51] M.M. Huber, S. Canonica, G.Y. Park, U. Von Gunten, Oxidation of pharmaceuticals during ozonation and advanced oxidation processes, Environ. Sci. Technol. 37 (2003) 1016–1024, https://doi.org/10.1021/es025896h.
[52] R. Gulde, B. Clerc, M. Rutsch, J. Helbing, E. Salhi, C.S. McArdell, U. von Gunten, Oxidation of 51 micropollutants during drinking water ozonation: Formation of transformation products and their fate during biological post-filtration, Water Res 207 (2021) 117812, https://doi.org/10.1016/j.watres.2021.117812.

[53] O.S. Keen, I. Ferrer, E. Michael Thurman, K.G. Linden, Degradation pathways of lamotrigine under advanced treatment by direct UV photolysis, hydroxyl radicals, and ozone, Chemosphere 117 (2014) 316–323, https://doi.org/10.1016/j.chemosphere.2014.07.085.
[54] X. Jin, S. Peldszus, P.M. Huck, Reaction kinetics of selected micropollutants in ozonation and advanced oxidation processes, Water Res 46 (2012) 6519–6530, https://doi.org/10.1016/j.watres.2012.09.026.
[55] B.A. Wols, C.H.M. Hofman-Caris, D.J.H. Harmsen, E.F. Beerendonk, Degradation of 40 selected pharmaceuticals by UV/H2O2, Water Res 47 (2013) 5876–5888, https://doi.org/10.1016/j.watres.2013.07.008.
[56] R. Gulde, B. Clerc, M. Rutsch, J. Helbing, E. Salhi, C.S. McArdell, U. von Gunten, Oxidation of 51 micropollutants during drinking water ozonation: Formation of transformation products and their fate during biological post-filtration, Water Res 207 (2021) 117812, https://doi.org/10.1016/j.watres.2021.117812.
[57] S.G. Zimmermann, A. Schmukat, M. Schulz, J. Benner, U. von Gunten, T. A. Ternes, Kinetic and mechanistic investigations of the oxidation of tramadol by ferrate and ozone, Environ. Sci. Technol. 46 (2012) 876–884, https://doi.org/10.1021/es203348q.
[58] Y. Lee, L. Kovalova, C.S. McArdell, U. von Gunten, Prediction of micropollutant elimination during ozonation of a hospital wastewater effluent, Water Res 64 (2014) 134–148, https://doi.org/10.1016/j.watres.2014.06.027.
[59] I. Zucker, H. Mamane, A. Riani, I. Gozlan, D. Avisar, Formation and degradation of N-oxide venlafaxine during ozonation and biological post-treatment, Sci. Total Environ. 619–620 (2018) 578–586, https://doi.org/10.1016/j.scitotenv.2017.11.133.
[60] B. Mathon, M. Coquery, Z. Liu, Y. Penru, A. Guillon, M. Esperanza, C. Miège, J.-M. Choubert, Ozonation of 47 organic micropollutants in secondary treated municipal effluents: Direct and indirect kinetic reaction rates and modelling, Chemosphere 262 (2021) 127969, https://doi.org/10.1016/j.chemosphere.2020.127969.
[61] R. Rosal, A. Rodríguez, J.A. Perdigón-Melón, A. Petre, E. García-Calvo, M. J. Gómez, A. Agüera, A.R. Fernández-Alba, Occurrence of emerging pollutants in urban wastewater and their removal through biological treatment followed by ozonation, Water Res 44 (2010) 578–588, https://doi.org/10.1016/j.watres.2009.07.004.
[62] G.A. Zoumpouli, F. Siqueira Souza, B. Petrie, L.A. Féris, B. Kasprzyk-Hordern, J. Wenk, Simultaneous ozonation of 90 organic micropollutants including illicit drugs and their metabolites in different water matrices, Environ. Sci. Water Res. Technol. 6 (2020) 2465–2478, https://doi.org/10.1039/D0EW00260G.
[63] F.J. Benitez, J.L. Acero, J.F. Garcia-Reyes, F.J. Real, G. Roldan, E. Rodriguez, A. Molina-Díaz, Determination of the reaction rate constants and decomposition mechanisms of ozone with two model emerging contaminants: DEET and nortriptyline, Ind. Eng. Chem. Res. 52 (2013) 17064–17073, https://doi.org/10.1021/ie402916u.
[64] W. Song, W.J. Cooper, B.M. Peake, S.P. Mezyk, M.G. Nickelsen, K.E. O'Shea, Free-radical-induced oxidative and reductive degradation of N,N′-diethyl-m-toluamide (DEET): Kinetic studies and degradation pathway, Water Res 43 (2009) 635–642, https://doi.org/10.1016/j.watres.2008.11.018.
[65] R. Broséus, S. Vincent, K. Aboulfadl, A. Daneshvar, S. Sauvé, B. Barbeau, M. Prévost, Ozone oxidation of pharmaceuticals, endocrine disruptors and pesticides during drinking water treatment, Water Res 43 (2009) 4707–4717, https://doi.org/10.1016/j.watres.2009.07.031.
[66] X. Shi, N.S. Dalal, A.C. Jain, Antioxidant behaviour of caffeine: Efficient scavenging of hydroxyl radicals, Food Chem. Toxicol. 29 (1991) 1–6, https://doi.org/10.1016/0278-6915(91)90056-D.
[67] C. Ye, X. Ma, J. Deng, X. Li, Q. Li, A.M. Dietrich, Degradation of saccharin by UV/H2O2 and UV/PS processes: A comparative study, Chemosphere 288 (2022), https://doi.org/10.1016/j.chemosphere.2021.132337.
[68] V. Maurino, M. Minella, F. Sordello, C. Minero, A proof of the direct hole transfer in photocatalysis: The case of melamine, Appl. Catal. 521 (2016) 57–67, https://doi.org/10.1016/j.apcata.2015.11.012.
[69] J.P. Pocostales, M.M. Sein, W. Knolle, C. von Sonntag, T.C. Schmidt, Degradation of ozone-refractory organic phosphates in wastewater by ozone and ozone/hydrogen peroxide (peroxone): The role of ozone consumption by dissolved organic matter, Environ. Sci. Technol. 44 (2010) 8248–8253, https://doi.org/10.1021/es1018288.
[70] C.D. Vecitis, H. Park, J. Cheng, B.T. Mader, M.R. Hoffmann, Treatment technologies for aqueous perfluorooctanesulfonate (PFOS) and perfluorooctanoate (PFOA), Front. Environ. Sci. Eng. China 3 (2009) 129–151, https://doi.org/10.1007/s11783-009-0022-7.
[71] A.M. Dreizler, E. Roduner, Reaction kinetics of hydroxyl radicals with model compounds of fuel cell polymer membranes, Fuel Cells 12 (2012) 132–140, https://doi.org/10.1002/fuce.201100157.
[72] H. Bader, J. Hoigné, Determination of ozone in water by the indigo method, Water Res 15 (1981) 449–456, https://doi.org/10.1016/0043-1354(81)90054-3.
[73] J.-C. Charpentier, Mass-transfer rates in gas-liquid absorbers and reactors, in: T. B. Drew, G.R. Cokelet, J.W. Hoopes, T. Vermeulen (Eds.), Advances in Chemical Engineering, Academic Press, 1981, pp. 1–133, https://doi.org/10.1016/S0065-2377(08)60025-3.
[74] C.R. Wilke, P. Chang, Correlation of diffusion coefficients in dilute solutions, AIChE J. 1 (1955) 264–270, https://doi.org/10.1002/aic.690010222.
[75] R. Sander, Compilation of Henry's law constants (version 5.0.0) for water as solvent, Atmos. Chem. Phys. 23 (2023) 10901–12440, https://doi.org/10.5194/acp-23-10901-2023.
[76] J. Ren, S. He, C. Ye, G. Chen, C. Sun, The ozone mass transfer characteristics and ozonation of pentachlorophenol in a novel microchannel reactor, Chem. Eng. J. 210 (2012) 374–384, https://doi.org/10.1016/j.cej.2012.09.011.
[77] D. Sauter, A. Dąbrowska, R. Bloch, M. Stapf, U. Miehe, A. Sperlich, R. Gnirss, T. Wintgens, Deep-bed filters as post-treatment for ozonation in tertiary municipal wastewater treatment: impact of design and operation on treatment goals, Environ. Sci. Water Res. Technol. 7 (2021) 197–211, https://doi.org/10.1039/D0EW00684J.
[78] J. Hollender, S.G. Zimmermann, S. Koepke, M. Krauss, C.S. McArdell, C. Ort, H. Singer, U. von Gunten, H. Siegrist, Elimination of organic micropollutants in a Municipal Wastewater Treatment Plant upgraded with a full-scale post-ozonation followed by sand filtration, Environ. Sci. Technol. 43 (2009) 7862–7869, https://doi.org/10.1021/es9014629.
[79] S. Naumov, G. Mark, A. Jarocki, C. von Sonntag, The reactions of nitrite ion with ozone in aqueous solution – new experimental data and Quantum-Chemical considerations, Ozone.: Sci. Eng. 32 (2010) 430–434, https://doi.org/10.1080/01919512.2010.522960.
[80] Y. Lee, D. Gerrity, M. Lee, A.E. Bogeat, E. Salhi, S. Gamage, R.A. Trenholm, E. C. Wert, S.A. Snyder, U. von Gunten, Prediction of micropollutant elimination during ozonation of Municipal Wastewater Effluents: Use of kinetic and water specific information, Environ. Sci. Tech. 47 (2013) 5872–5881, https://doi.org/10.1021/es400781r.
[81] S. Kharel, M. Stapf, U. Miehe, M. Ekblad, M. Cimbritz, P. Falås, J. Nilsson, R. Sehlén, J. Bregendahl, K. Bester, Removal of pharmaceutical metabolites in wastewater ozonation including their fate in different post-treatments, Sci. Total Environ. 759 (2021) 143989, https://doi.org/10.1016/j.scitotenv.2020.143989.
[82] A. Cruz-Alcalde, S. Esplugas, C. Sans, Abatement of ozone-recalcitrant micropollutants during municipal wastewater ozonation: Kinetic modelling and surrogate-based control strategies, J. Chem. Eng. 360 (2019) 1092–1100, https://doi.org/10.1016/j.cej.2018.10.206.
[83] J. Hoigné, H. Bader, Rate constants of reactions of ozone with organic and inorganic compounds in water: non-dissociating organic compounds, Water Res 17 (1983) 173–183, https://doi.org/10.1016/0043-1354(83)90098-2.
[84] L.T. Phan, H. Schaar, E. Saracevic, J. Krampe, N. Kreuzinger, Effect of ozonation on the biodegradability of urban wastewater treatment plant effluent, Sci. Total Environ. 812 (2022) 152466, https://doi.org/10.1016/j.scitotenv.2021.152466.
[85] A. Schmitt, J. Mendret, H. Cheikho, S. Brosillon, Ozone diffusion through a hollow fiber membrane contactor for pharmaceuticals removal and bromate minimization, Membr. (Basel) 13 (2023) 171, https://doi.org/10.3390/membranes13020171.
[86] J. Hoigne, H. Bader, Ozonation of water: kinetics of oxidation of ammonia by ozone and hydroxyl radicals, Environ. Sci. Tech. 12 (1978) 79–84, https://doi.org/10.1021/es60137a005.
[87] G.A. de Vera, W. Gernjak, H. Weinberg, M.J. Farré, J. Keller, U. von Gunten, Kinetics and mechanisms of nitrate and ammonium formation during ozonation of dissolved organic nitrogen, Water Res 108 (2017) 451–461, https://doi.org/10.1016/j.watres.2016.10.021.
[88] P.C. Singer, W.B. Zilli, Ozonation of ammonia in wastewater, Water Res 9 (1975) 127–134, https://doi.org/10.1016/0043-1354(75)90001-9.
[89] B. Hickel, K. Sehested, Reaction of hydroxyl radicals with ammonia in liquid water at elevated temperatures, Radiat. Phys. Chem. 39 (1992) 355–357, https://doi.org/10.1016/1359-0197(92)90244-A.
[90] E.Y. Ordóñez, J.B. Quintana, R. Rodil, R. Cela, Determination of artificial sweeteners in water samples by solid-phase extraction and liquid chromatography–tandem mass spectrometry, J. Chromatogr. A 1256 (2012) 197–205, https://doi.org/10.1016/j.chroma.2012.07.073.
[91] H. An, X. Li, Q. Yang, D. Wang, T. Xie, J. Zhao, Q. Xu, F. Chen, Y. Zhong, Y. Yuan, G. Zeng, The behavior of melamine in biological wastewater treatment system, J. Hazard. Mater. 322 (2017) 445–453, https://doi.org/10.1016/j.jhazmat.2016.10.036.
[92] H. Zhu, K. Kannan, Occurrence and distribution of melamine and its derivatives in surface water, drinking water, precipitation, wastewater, and swimming pool water, Environ. Pollut. 258 (2020) 113743, https://doi.org/10.1016/j.envpol.2019.113743.
[93] L.H. Lütjens, S. Pawlowski, M. Silvani, U. Blumenstein, I. Richter, Melamine in the environment: a critical review of available information, Environ. Sci. Eur. 35 (2023) 2, https://doi.org/10.1186/s12302-022-00707-y.
[94] A. Ladhari, G. La Mura, C. Di Marino, G. Di Fabio, A. Zarrelli, Sartans: What they are for, how they degrade, where they are found and how they transform, Sustain. Chem. Pharm. 20 (2021) 100409, https://doi.org/10.1016/j.scp.2021.100409.
[95] Medicine Infarmed, Healthcare Products Statistics, (2018). https://www.infarmed.pt/documents/15786/3729736/Estatística+do+medicamento+%202018/bc5b3951-7d33-3374-f883-29e72d6b9013?version=%201.0.
[96] L. Pang, A.G.L. Borthwick, E. Chatzisymeon, Determination, occurrence, and treatment of saccharin in water: a review, J. Clean. Prod. 270 (2020) 122337, https://doi.org/10.1016/j.jclepro.2020.122337.
[97] S.S. Lakade, Q. Zhou, A. Li, F. Borrull, N. Fontanals, R.M. Marcé, Hypercrosslinked particles for the extraction of sweeteners using dispersive solid-phase extraction from environmental samples, J. Sep. Sci. 41 (2017) 1618–1624, https://doi.org/10.1002/jssc.201701113.
[98] R. Li, C. Liang, S.B. Svendsen, V. Kisielius, K. Bester, Sartan blood pressure regulators in classical and biofilm wastewater treatment – Concentrations and metabolism, Water Res 229 (2023) 119352, https://doi.org/10.1016/j.watres.2022.119352.

[99] E.C. Wert, S. Gonzales, M.M. Dong, F.L. Rosario-Ortiz, Evaluation of enhanced coagulation pretreatment to improve ozone oxidation efficiency in wastewater, Water Res 45 (2011) 5191–5199, https://doi.org/10.1016/j.watres.2011.07.021.
[100] L. Kovalova, H. Siegrist, U. von Gunten, J. Eugster, M. Hagenbuch, A. Wittmer, R. Moser, C.S. McArdell, Elimination of micropollutants during post-treatment of hospital wastewater with powdered activated carbon, ozone, and UV, Environ. Sci. Technol. 47 (2013) 7899–7908, https://doi.org/10.1021/es400708w.
[101] C. Zwiener, F. Frimmel, Oxidative treatment of pharmaceuticals in water, Water Res 34 (2000) 1881–1885, https://doi.org/10.1016/S0043-1354(99)00338-3.
[102] R. Guillossou, J. Le Roux, S. Brosillon, R. Mailler, E. Vulliet, C. Morlay, F. Nauleau, V. Rocher, J. Gaspéri, Benefits of ozonation before activated carbon adsorption for the removal of organic micropollutants from wastewater effluents, Chemosphere 245 (2020) 125530, https://doi.org/10.1016/j.chemosphere.2019.125530.
[103] R.L. Oulton, T. Kohn, D.M. Cwiertny, Pharmaceuticals and personal care products in effluent matrices: a survey of transformation and removal during wastewater treatment and implications for wastewater management, J. Environ. Monit. 12 (2010) 1956, https://doi.org/10.1039/c0em00068j.
[104] M. Marce, B. Domenjoud, S. Esplugas, S. Baig, Ozonation treatment of urban primary and biotreated wastewaters: Impacts and modeling, Chem. Eng. J. 283 (2016) 768–777, https://doi.org/10.1016/j.cej.2015.07.073.
[105] E.R. Toroz, Y. Akdag, M. Fakioglu, S. Korkut, E. Sagir Kurt, E. Atli, H. Guven, H. Ozgun, I. Ozturk, M.E. Ersahin, Effects of ozone dose and contact time on ozonation process performance for treatment of high rate activated sludge process effluent, Ozone.: Sci. Eng. 45 (2023) 431–445, https://doi.org/10.1080/01919512.2022.2157243.
[106] S.K. Stylianou, S.D. Sklari, D. Zamboulis, V.T. Zaspalis, A.I. Zouboulis, Development of bubble-less ozonation and membrane filtration process for the treatment of contaminated water, J. Membr. Sci. 492 (2015) 40–47, https://doi.org/10.1016/j.memsci.2015.05.036.